KIER DISCUSSION PAPER SERIES

KYOTO INSTITUTE
OF
ECONOMIC RESEARCH

Discussion Paper No. 929

Agglomerations in a multi-region economy:
Poly-centric versus mono-centric patterns

Takashi Akamatsu, Tomoya Mori, and Yuki Takayama

October 2015

KYOTO UNIVERSITY

KYOTO, JAPAN

Agglomerations in a multi-region economy: Poly-centric versus mono-centric patterns*

Takashi Akamatsu†, Tomoya Mori‡, and Yuki Takayama§

October 21, 2015

Abstract

Agglomeration externalities have been recognized as major sources of lumpy spatial distributions of industries and population. While the abstraction of interregional space has been a common exercise, recent increasing availability of disaggregated geographical data and more sophisticated computational techniques have promoted counterfactual analyses based on many-region models of agglomeration externalities with explicit interregional space (e.g., Redding and Sturm, 2008; Allen and Arkolakis, 2014). A caveat is that incorporating interregional space to a many-region model with agglomeration externalities does not by itself warrant the formation of poly-centric agglomerations in stable equilibria—a crucial property in order to replicate the observed geography of agglomerations. We elaborate this point by comparing a pair of new economic geography models, Forslid and Ottaviano (2003) and Helpman (1998). In a two-region economy, these models exhibit both "agglomeration" (i.e., a relative concentration of mobile agents in one of the regions) and "dispersion" (i.e., a uniform distribution of mobile agents across the two regions). But, if the location space were more disaggregated, only the former admits poly-centric agglomerations in stable equilibria, while in the latter, only a mono-centric agglomeration can occur if any.

Keywords: new economic geography model, many-region model, multiple agglomerations, stability, bifurcation

JEL Classification: R12, R13, F15, F22, C62

---

*We are grateful for the comments and suggestions made by Marcus Berliant, Masahisa Fujita, Kiyohiro Ikeda, Se-il Mun, Yasusada Murata, Minoru Osawa, Toshimori Otazawa, Daisuke Oyama, Yasuhiro Sato, Takatoshi Tabuchi, Kazuhiro Yamamoto, and Dao-Zhi Zeng, as well as participants at the 23th Applied Regional Science Conference Meeting in Yamagata. We greatly acknowledge the funding from the Japan Society for the Promotion of Science, Grant-in-Aid for Scientific Research (B) 25285074, Grant-in-Aid for Challenging Exploratory Research 15K14044, and Grant-in-Aid for Young Scientists (B) 15K18136.

†Graduate School of Information Sciences, Tohoku University, 6-6-06 Aoba, Aramaki, Aoba-ku, Sendai 980-8579, Japan. Tel(Fax) +81-22-795-7505, e-mail: akamatsu@plan.civil.tohoku.ac.jp

‡Institute of Economic Research, Kyoto University, Yoshida-honmachi, Sakyo-ku, Kyoto 606-8501, Japan.

§Graduate School of Engineering, Tohoku University, 6-6-06 Aoba, Aramaki, Aoba-ku, Sendai 980-8579, Japan. e-mail: takayama@civil.tohoku.ac.jp

1 Introduction

Empirical studies in the recent decades have accumulated ample evidence that agglomeration externalities are major sources of lumpy spatial distributions of industries and population (see, e.g., Rosenthal and Strange, 2004, for a survey). Accordingly a wide variety of formal models for the underlying mechanisms have been proposed (see, e.g., Duranton and Puga, 2004, for a survey). Nevertheless, there is little theoretical development to account for the *global spatial patterns* of agglomerations, and consequently the empirical studies so far have focused mainly on the *local interactions* between the agglomeration size and location-specific factors (see, e.g., Combes and Gobillon, 2015, for a survey).

A main reason for this is that the explicit consideration of interregional space is a primary obstacle for achieving analytical tractability in theoretical models. There are two popular approaches adopted to abstract from interregional space. One is the so-called "city-systems" framework which was first proposed by Henderson (1974). The models of this type explain the diversity among cities with respect to, e.g., productivity, growth, the composition of industries and population, in terms of the tension between city-specific positive and negative externalities together with other local factors, while abstracting from inter-city space (see Behrens and Robert-Nicoud, 2015, for a survey). The other is to consider the minimum spatial economy consist of two regions in which the agglomeration is expressed simply in terms of the concentration of mobile agents in one of the two regions. As one exception, the new economic geography (NEG) was developed in 1990s to explore the spatial patterns of agglomerations in a general location space (e.g., Fujita et al., 1999, Pt. II). But, this approach has never flourished, and the two-region setup soon dominated the NEG literature (see, e.g., Baldwin et al., 2003).

While the disregard of interregional space has been routine in the theoretical modeling of spatial economy, the recent increasing availability of disaggregated geographical data and sophisticated computational techniques have promoted the emergence of counterfactual analyses based on many-region models with agglomeration externalities and explicit interregional space (see Redding and Sturm, 2008; Desmet and Rossi-Hansberg, 2009, 2014, 2015; Allen and Arkolakis, 2014; Behrens et al., 2014; Redding, 2015; Desmet et al., 2015a,b). This shift took place rather suddenly, without close inspection of the model behavior in a many-region economy. Among a number of requirements for these models, the most fundamental one perhaps is the ability to endogenously generate polycentric agglomerations in stable equilibria. A caveat is that incorporating interregional space to a many-region model with agglomeration externalities does not by itself warrant this consequence.

We elaborate this point by comparing a pair of NEG models as they offer us a tractability in a multi-region setup. The first one is a multi-region extension of the two-region NEG model developed by Forslid and Ottaviano (2003) (henceforth called "FO model"), which is a solvable variant of the original core-periphery model by Krugman (1991). The

other is a multi-region version of Helpman (1998) (henceforth "Hm model") in which the agricultural sector in the core-periphery model is replaced with the housing sector.[1] In a two-region economy, these models exhibit both "agglomeration" (i.e., a relative concentration of mobile agents in one of the two regions) and "dispersion" (i.e., a uniform distribution of mobile agents across the regions). But in a multi-region economy with more than two regions, only the former can generate poly-centric agglomerations in stable equilibria, while in the latter, only a mono-centric agglomeration can occur if any. That is, even if the Hm model were extended to a many-region economy, it will not be able to replicate poly-centric agglomerations.

In fact, Redding and Sturm (2008) calibrated the multi-region Hm model to fit the population agglomeration pattern in Germany in 1939. But, nearly 90% of the actual city size variation was accounted for by the *unobserved city-specific amenities* that were given *exogenously* to the model.[2] This is not surprising provided that the poly-centric city system in Germany is hardly represented by a mono-centric pattern which is the only possible agglomeration pattern in the Hm model. Fabinger (2015) pointed out that mono-centric patterns are the only possibility in stable equilibria also in the model by Allen and Arkolakis (2014) which was calibrated to fit the spatial population distribution in the US.

To this end, we apply the analytical approach developed by Akamatsu et al. (2012) that exploited the circulant property of the "spatial discounting matrix (SDM)" in a circular region system ("racetrack economy (RE)") and the "discrete Fourier transformation (DFT)." Their approach is applicable to various types of NEG models with an arbitrary discrete number of symmetric locations, and allows us not only to examine whether the agglomeration of mobile factors emerges from a uniform distribution but also to trace the *evolution* of spatial agglomeration patterns (i.e., bifurcations from various *poly-centric patterns* as well as from a uniform pattern) in response to the change in parameter values.

In this article, these tools are utilized to elaborate the dichotomy of the model behavior between the FO- and Hm-models under the multi-region extension. For each of these multi-region models with symmetric locations (i.e., equidistant locations placed on a circumference and unskilled labor/land supply are symmetrically distributed),[3] we first derive (in Proposition 3.1) the indirect utility of a consumer for a short-run equilibrium (in which a location pattern of consumers is fixed) as a function of mobile consumers'

[1] The urban costs modeled in Tabuchi (1998) and Murata and Thisse (2005) exercise a similar effect on agglomeration patterns as the housing sector in the Hm model.

[2] More precisely, the unobserved amenities in their model is the city-specific "housing stock" in the original Hm model which acts as a slack variable to fill the gap between the actual and model city sizes. If the log of city sizes are regressed on their "unobserved amenity" in 1939 (provided in their online Appendix), the fit is as high as $R^2 = 0.895$. See also Nakajima (2008) and Redding (2015) for similar applications of the Hm model.

[3] It is worth noting that, in many fields such as physics, engineering, and applied mathematics, the concept that bifurcation behavior under symmetry assumption reveals essential properties of the model has been recognized, and the symmetry assumption has become the orthodox and powerful tool to clarify the intrinsic properties of many phenomena (e.g., Golubitsky et al., 1988; Ikeda and Murota, 2010; Stewart, 2013; Strogatz, 2014).

spatial distribution. In order to understand the bifurcation mechanism of the models, we need to understand how the eigenvalues of the Jacobian matrix of the adjustment process[4] (that is a function of the indirect utility) for each model depend on bifurcation parameters (e.g., the transportation cost parameter). A combination of the RE (with discrete locations) and the resultant circulant properties of the SDM greatly facilitate this analysis. Indeed, it is shown (in Proposition 4.1) that the k-th eigenvalue g_k of the Jacobian matrix of the adjustment process can be expressed as a simple unimodal function of the k-th eigenvalue f_k of the SDM. The former eigenvalue g_k thus obtained has a natural economic interpretation as the strength of *"net agglomeration force,"* and offers the key to understanding the agglomeration properties of the NEG models. In this bifurcation analysis, we intentionally restricted ourselves to the four-region economy for clarity of exposition, as it allows us to illustrate the essential features of our approach without going into excessive technical detail.[5]

Exploiting the information on the eigenvalues thus obtained, we investigate each of the evolutionary processes of the spatial agglomeration of mobile factors in the multi-region FO model and the Hm model in turn. In the investigation, we follow the process of agglomeration from a uniform distribution over the regions, since it is natural from the bifurcation theoretical viewpoint to follow (possibly) a series of bifurcations in such a way that the symmetry is successively reduced.[6]

For the FO model, we consider the process in which transportation costs steadily decrease over time. Starting from the infinite transport costs at which the uniform distribution of mobile factors over the regions is a unique stable equilibrium, we investigate when and what spatial patterns of agglomeration emerge (i.e., bifurcation occurs) with the decrease in transport costs. The analytical expression of the eigenvalues allows us to identify the "break point" at which the bifurcation occurs, and the associated patterns of agglomeration that emerge at the bifurcation (Proposition 5.2). Unlike the conventional two-region models that exhibit only a single bifurcation, this is not the end of the story in the four-region model. Indeed, it is shown (in Proposition 5.3) that the agglomeration pattern after the first bifurcation evolves over time with steady decrease in transport costs; it first grows to a duo-centric pattern, which continues to be stable for a while. Further decrease in transport costs, however, trigger the second bifurcation, which in turn leads to the formation of a mono-centric agglomeration.

For the Hm model, in contrast to the FO model, we consider the process in which transport cost steadily increase from the minimum value, 0, at which a uniform distribution over the regions is a unique stable equilibrium. By the eigenvalue analysis similar

[4] In this paper, we employ the replicator dynamic as the adjustment process.

[5] The approach presented in this paper can deal with a model with an arbitrary number of regions (refer to Akamatsu et al., 2012). Note that this approach allows us to obtain stable equilibrium agglomeration patterns even if the model exhibits hysteresis. Furthermore, by identifying the type of bifurcation (supercritical or subcritical) using the approach presented in Ikeda and Murota (2010, 2014), we can check whether hysteresis exists.

[6] This strategy is commonly used in various fields of science to study bifurcation behavior of symmetric systems (e.g., Golubitsky et al., 1988; Ikeda and Murota, 2010; Stewart, 2013; Strogatz, 2014).

to that for the FO model, it is shown (in Proposition 6.2) that a uniform distribution directly branches to a mono-centric distribution. Furthermore, it is also proved that the duo-centric pattern, which emerges in the FO model, never emerges in the Hm model (Proposition 6.3). That is, unlike the FO model, the Hm model admits at most a single peak in spatial distribution of mobile agents, even if it involves more than two regions.

The remainder of the paper is organized as follows. Section 2 reviews the related literature. Section 3 presents the equilibrium conditions of the multi-region NEG models as well as definitions of the stability and bifurcation of the equilibrium state. Section 4 defines the SDM in a racetrack economy, whose eigenvalues are provided by a DFT. Sections 5 and 6 analyze the evolutionary process of spatial patterns observed in the FO and Hm models, respectively. These theoretical results are then illustrated by numerical examples in Section 7. Finally, Section 8 concludes the paper.

2 Related literature

A method that can be used to analytically predict bifurcation properties of a wide class of multi-region models is the Turing (1952) approach, in which one focuses on the onset of instability in the uniform equilibrium distribution ("flat earth equilibrium") of mobile agents. That is, by assuming a certain class of adjustment process (e.g., *"replicator dynamic"*), one examines a trend of the economy away from, rather than toward, the flat earth equilibrium whose instability implies the *emergence* of *some* agglomeration.[7] Krugman (1996) and Fujita et al. (1999, Chap.6) applied this approach to the NEG model with a continuum of locations on the circumference and succeeded in showing that a steady decrease in transportation costs leads toward the instability of the flat earth equilibrium state. Subsequently, a few studies have also applied this approach, and re-examined the robustness of Krugman's findings in the core-periphery model with a continuous space racetrack economy. Mossay (2003) theoretically qualified Krugman's results in the case of workers' heterogeneous preferences for location. Picard and Tabuchi (2010) examined the impact of the shape of transport costs on the structure of spatial equilibria. While this approach offers a remarkable way of thinking about a seemingly complex issue, it deals with only the first stage of agglomeration when the value of a parameter (e.g., transportation cost) steadily changes. Therefore, it cannot provide a good description of what actually happens thereafter. Indeed, Krugman (1996) and Fujita et al. (1999, Chap.17) resorted to rather ad hoc numerical simulations for analyzing the possible bifurcations in the later stages; subsequent studies of Mossay (2003) and Picard and Tabuchi (2010) were silent on such bifurcations.

Tabuchi et al. (2005) presented an approach to study the impact of decreasing transportation costs on the size and number of locations in the multi-region model that extends a two-region NEG model by Ottaviano et al. (2002). Oyama (2009) showed that

[7]The first notable application of this approach to analyzing agglomeration in a spatial economy was made by Papageorgiou and Smith (1983).

the multi-region NEG model admits a potential function, which allows identifying a stationary state that is uniquely absorbing and globally accessible under perfect foresight dynamics. However, these analyses were restricted to a very special class of transport geometry: Tabuchi et al. (2005) assumed that locations are equidistant (i.e., transportation costs are the same regardless of the origin and destination); Oyama (2009) allowed different locations to have different destination specific transportation costs but which are independent of the origin. Recently, Tabuchi and Thisse (2011) showed that a hierarchical urban system structure emerges for the Pflüger (2004) model with multiple industries. Although they analyzed the multi-region NEG model, the purpose and the emphasis of their study was to show how a hierarchical urban system structure emerges for the NEG model with multiple industries, and not to provide a general methodology that is applicable to the analysis of a wider class of models other than Pflüger (2004) model.[8]

Akamatsu et al. (2012) provides an analytical approach to study the evolution of spatial agglomeration patterns with changes in the parameter values and analyzes the multi-region NEG model by Pflüger (2004). Although this approach is applicable to various types of NEG models, their focus is to analytically prove the occurrence of "spatial period-doubling cascade" in Pflüger's model with 2^n regions. Ikeda et al. (2012a) utilizes group-theoretic bifurcation theory to study the bifurcation behavior of multi-region NEG models. While this theory can narrow down the possible bifurcation patterns to occur for a more general location space (e.g., two-dimensional discrete location spaces in Ikeda et al. (2012b, 2014) and Ikeda and Murota (2014)) than that in the present study, it cannot pin down an explicit event to occur, i.e., the stability of the agglomeration patterns cannot be identified. Hence, it must resort to the numerical analysis to examine what agglomeration patterns emerge as stable equilibria.

3 The Model

3.1 Basic Assumptions

We present a pair of multi-region NEG models whose frameworks follow Forslid and Ottaviano (2003) and Helpman (1998) (defined as FO and Hm, respectively).[9]

3.1.1 Forslid and Ottaviano (2003) Model

We first provide basic assumptions of the FO model. The economy is composed of K regions indexed by $i = 0, 1, ..., K-1$, two factors of production and two sectors. The two factors of production are skilled and unskilled labor while the workers supply one unit of each type of labor inelastically. The total endowment of skilled and unskilled workers

[8]The analysis of Tabuchi and Thisse (2011) covers only a limited range of parameter values in which bifurcations are supercritical. Hence, it does not provide the entire description of bifurcation behavior of even the Pflüger model.

[9]Ottaviano (2001) presents the same model as Forslid and Ottaviano (2003), which is based on Forslid (1999) and Ottaviano (1996).

is H and L, respectively. The skilled worker is mobile across regions and h_i denotes their population in region i. The unskilled worker is immobile, and the population in region i is denoted by l_i. The two sectors consist of agriculture (abbreviated as A) and manufacturing (abbreviated as M). The A-sector output is homogeneous and each unit is produced using a unit of unskilled labor under perfect competition. This output is chosen to be the numèraire. The M-sector output is a horizontally differentiated product that is produced using both skilled and unskilled labor under increasing returns to scale and Dixit-Stiglitz monopolistic competition. The goods of both sectors are transported, but the transportation of A-sector goods is frictionless while the transportation of M-sector goods is inhibited by iceberg transportation costs. That is, for each unit of M-sector goods transported from region i to j, only a fraction $1/\tau_{ij} < 1$ arrives.

All workers have identical preferences U over both M- and A-sector goods. The utility of an individual in region i is given by

$$U(C_i^{\mathrm{M}}, C_i^{\mathrm{A}}) = \mu \ln C_i^{\mathrm{M}} + (1-\mu) \ln C_i^{\mathrm{A}} \quad (0 < \mu < 1), \tag{3.1}$$

$$C_i^{\mathrm{M}} \equiv \left(\sum_j \int_0^{n_j} q_{ji}(k)^{(\sigma-1)/\sigma} dk \right)^{\sigma/(\sigma-1)}, \tag{3.2}$$

where C_i^{A} is the consumption of A-sector goods in region i; C_i^{M} represents the manufacturing aggregate in region i; $q_{ji}(k)$ is the consumption of variety $k \in [0, n_j]$ produced in region j and n_j is the number of varieties produced in region j; μ is the constant expenditure share on industrial varieties and σ is the constant elasticity of substitution between any two varieties. The budget constraint is given by

$$C_i^{\mathrm{A}} + \sum_j \int_0^{n_j} p_{ji}(k) q_{ji}(k) dk = y_i, \tag{3.3}$$

where $p_{ji}(k)$ denotes the price in region i of the M-sector goods produced in region j, and y_i denotes the income of an individual in region i. The incomes (wages) of the skilled and the unskilled workers are represented, respectively, by w_i and w_i^{u}.

The utility maximization of (3.1) yields the following demand $q_{ji}(k)$ of an individual in region i for a variety of M-sector goods k produced in region j:

$$q_{ji}(k) = \frac{\mu \{p_{ji}(k)\}^{-\sigma}}{\rho_i^{1-\sigma}} y_i, \tag{3.4}$$

$$\rho_i \equiv \left(\sum_j \int_0^{n_j} p_{ji}(k)^{1-\sigma} dk \right)^{1/(1-\sigma)}, \tag{3.5}$$

where ρ_i denotes the price index of the differentiated product in region i. Since the total

income in region i is $w_i h_i + w_i^{\mathrm{u}} l_i$, we have the total demand $Q_{ji}(k)$:

$$Q_{ji}(k) = \frac{\mu\{p_{ji}(k)\}^{-\sigma}}{\rho_i^{1-\sigma}}(w_i h_i + w_i^{\mathrm{u}} l_i). \tag{3.6}$$

In the M-sector, product differentiation ensures a one-to-one relationship between firms and varieties. Specifically, in order to produce $x_i(k)$ unit of product k, a firm incurs a fixed input requirement of α unit of skilled labor and a marginal input requirement of $\beta x_i(k)$ unit of unskilled labor. Therefore, the total cost of production for a firm in region i is thus given by $\alpha w_i + \beta x_i(k) w_i^{\mathrm{u}}$. A-sector technology requires one unit of unskilled labor to produce one unit of output. With free trade in the A-sector, the choice of these goods as the numèraire implies that in equilibrium, the wage of the unskilled worker w_i^{u} is equal to one in all regions, i.e., $w_i^{\mathrm{u}} = 1$.[10]

Due to the iceberg transportation costs, the total supply of the M-sector firm in region i (i.e., $x_i(k)$) is given by

$$x_i(k) = \sum_j \tau_{ij} Q_{ij}(k). \tag{3.7}$$

Therefore, a typical M-sector firm located in region i maximizes profit as given by:

$$\Pi_i(k) = \sum_j p_{ij}(k) Q_{ij}(k) - \left(\alpha w_i + \beta \sum_j \tau_{ij} Q_{ij}(k) \right). \tag{3.8}$$

Since we have a continuum of firms, each one is negligible in the sense that its action has no impact on the market (i.e., the price indices). Hence, the first order condition for profit maximization gives

$$p_{ij}(k) = \frac{\sigma\beta}{\sigma - 1}\tau_{ij}. \tag{3.9}$$

This expression implies that the price of M-sector goods does not depend on variety k, so that $Q_{ij}(k)$ and $x_i(k)$ also do not depend on k. Therefore, we describe these variables without argument k.

3.1.2 Helpman (1998) Model

We next present a multi-region Hm model. Helpman (1998) introduces the housing (abbreviated as H) sector that works as a centrifugal force instead of the A-sector in Krugman (1991), and thereby assumes that all workers are mobile and each region i has a fixed stock A_i of housing.

[10] Wage equalization holds as long as the A-sector goods are produced in all regions. We assume that this condition is satisfied; therefore, $\beta x_i n_i < l_i \ \forall i$ holds.

The utility of a worker in region i is expressed as

$$U(C_i^{\mathrm{M}}, C_i^{\mathrm{H}}) = \mu \ln C_i^{\mathrm{M}} + (1-\mu) \ln C_i^{\mathrm{H}} \quad (0 < \mu < 1), \tag{3.10}$$

where C_i^{H} is the consumption of H-sector goods in region i and C_i^{M} denotes the manufacturing aggregate in region i, which is given by (3.2). The budget constraint of a worker located at i is represented by

$$p_i^{\mathrm{H}} C_i^{\mathrm{H}} + \sum_j \int_0^{n_j} p_{ji}(k) q_{ji}(k) dk = y_i, \tag{3.11}$$

where p_i^{H} is the price of H-sector goods in region i. The utility maximization of (3.10) leads to the following demand:

$$C_i^{\mathrm{M}} = \mu \frac{y_i}{\rho_i}, \tag{3.12}$$

$$C_i^{\mathrm{H}} = (1-\mu) \frac{y_i}{p_i^{\mathrm{H}}}, \tag{3.13}$$

$$Q_{ji}(k) = \frac{\mu \{p_{ji}(k)\}^{-\sigma}}{\rho_i^{1-\sigma}} y_i h_i. \tag{3.14}$$

We assume that the housing stocks are equally owned by all workers as in Helpman (1998) and Pflüger and Südekum (2010).[11] Therefore, the income of a worker is composed of labor income w_i plus income $\bar{w}$ from the housing ownership

$$y_i = w_i + \bar{w}, \tag{3.15a}$$

$$\bar{w} = \frac{1}{H} \sum_j p_j^{\mathrm{H}} C_j^{\mathrm{H}} h_j. \tag{3.15b}$$

In order to normalize prices, we set $\bar{w}$ equal to unity.

In the H-sector, the total demand $h_i C_i^{\mathrm{H}}$ in region i cannot be greater than the maximum supply A_i. If the demand in region i is less than the supply, the price p_i^H should be the lower boundary (i.e., zero), otherwise positive. Thus, we have the following housing market clearing condition:

$$\begin{cases} h_i C_i^{\mathrm{H}} = A_i & \text{if} \quad p_i^{\mathrm{H}} > 0, \\ h_i C_i^{\mathrm{H}} \leq A_i & \text{if} \quad p_i^{\mathrm{H}} = 0, \end{cases} \quad \forall i. \tag{3.16}$$

[11] Ottaviano et al. (2002), Murata and Thisse (2005), and Redding and Sturm (2008) assume that the housing stocks are locally owned (i.e., $\bar{w}_i = p_i^{\mathrm{H}} C_i^{\mathrm{H}}$). Note that the income of a worker is given by $y_i = w_i/\mu$ under this assumption. This implies that the specification of housing ownership will not affect the essential results obtained in this study.

This condition and (3.13) give the consumption of housing and its price in region i:

$$C_i^{\mathrm{H}} = \frac{A_i}{h_i}, \tag{3.17}$$

$$p_i^{\mathrm{H}} = (1-\mu)\frac{y_i h_i}{A_i}. \tag{3.18}$$

In the M-sector, a firm requires $\alpha + \beta x_i(k)$ unit of (skilled) labor input for producing $x_i(k)$ unit of variety k. The profit of a firm is then represented by

$$\Pi_i(k) = \sum_j p_{ij}(k)Q_{ij}(k) - w_i\left(\alpha + \beta x_i(k)\right), \tag{3.19}$$

which is almost the same as that of the FO model except for the cost function. Furthermore, the market clearing condition for M-sector goods is expressed by (3.7). Therefore, the profit maximization yields $p_{ij}(k)$ as follows.

$$p_{ij}(k) = \frac{\sigma\beta}{\sigma-1} w_i \tau_{ij}. \tag{3.20}$$

This expression implies that as in the FO model, the price of M-sector goods does not depend on variety k, and thus we describe the variables without argument k.

3.2 Short-Run Equilibrium

In the short run, the skilled workers are immobile between regions; that is, their spatial distribution ($\boldsymbol{h} \equiv [h_0, h_1, ..., h_{K-1}]^\top$) is taken as given. The short-run equilibrium conditions consist of the M-sector goods market clearing condition, the zero profit condition due to the free entry and exit of firms, and the skilled labor market clearing condition. The first condition can be written as (3.7). The second condition requires that the operating profit of a firm is entirely absorbed by the wage bills of its skilled workers:

$$\text{[FO model]} \quad w_i = \frac{1}{\alpha}\left(\sum_j p_{ij}Q_{ij} - \beta x_i\right), \tag{3.21a}$$

$$\text{[Hm model]} \quad w_i\left(\alpha + \beta x_i\right) = \sum_j p_{ij}Q_{ij}. \tag{3.21b}$$

The third condition is represented as

$$\text{[FO model]} \quad \alpha n_i = h_i, \tag{3.22a}$$

$$\text{[Hm model]} \quad (\alpha + \beta x_i) n_i = h_i. \tag{3.22b}$$

Equations (3.9), (3.20), (3.21), and (3.22) give the price index ρ_i of the FO and Hm models

as follows:

$$\text{[FO model]} \quad \rho_i = \frac{\sigma\beta}{\sigma-1}\left(\frac{1}{\alpha}\sum_j h_j d_{ji}\right)^{1/(1-\sigma)}, \tag{3.23a}$$

$$\text{[Hm model]} \quad \rho_i = \frac{\sigma\beta}{\sigma-1}\left(\frac{1}{\alpha\sigma}\sum_j w_j^{1-\sigma} h_j d_{ji}\right)^{1/(1-\sigma)}, \tag{3.23b}$$

where $d_{ji} \equiv \tau_{ji}^{1-\sigma}$ is a *"spatial discounting factor"* between region i and j. Furthermore, substituting (3.6), (3.7), (3.9), (3.14), (3.20), and (3.23) into (3.21), we have the short-run equilibrium wage equations:

$$\text{[FO model]} \quad w_i = \frac{\mu}{\sigma}\sum_j \frac{d_{ij}}{\Delta_j}(w_j h_j + l_j), \tag{3.24a}$$

$$\text{[Hm model]} \quad w_i = \mu\sum_j \frac{d_{ij} w_i^{1-\sigma}}{\tilde{\Delta}_j}(w_j + 1)h_j, \tag{3.24b}$$

where $\Delta_j \equiv \sum_k d_{kj} h_k$ and $\tilde{\Delta}_j \equiv \sum_k d_{kj} w_k^{1-\sigma} h_k$.

To obtain the indirect utility function $v_i(\boldsymbol{h})$ of these models, we express the equilibrium wage $w_i(\boldsymbol{h})$. For this, we rewrite (3.24) in matrix form by using the *"spatial discounting matrix"* $\boldsymbol{D}$ whose (i, j) element is d_{ij}. Then, the equilibrium wage equations (3.24) are represented as

$$\text{[FO model]} \quad \boldsymbol{w} = \kappa\left[\boldsymbol{I} - \kappa\boldsymbol{M}\text{diag}[\boldsymbol{h}]\right]^{-1}\boldsymbol{M}\boldsymbol{l}, \tag{3.25a}$$

$$\text{[Hm model]} \quad (\text{diag}[\tilde{\boldsymbol{w}}])^{\sigma}\mathbf{1} = \mu\tilde{\boldsymbol{M}}\text{diag}[\boldsymbol{h}](\tilde{\boldsymbol{w}} + \mathbf{1}), \tag{3.25b}$$

where $\kappa \equiv \mu/\sigma$, $\boldsymbol{l} \equiv [l_0, l_1, ..., l_{K-1}]^\top$, $\mathbf{1} \equiv [1, 1, ..., 1]^\top$, and $\boldsymbol{I}$ is a unit matrix. $\boldsymbol{w}$ and $\tilde{\boldsymbol{w}}$ denote the equilibrium wages of the FO and Hm models, respectively. $\boldsymbol{M}$ and $\tilde{\boldsymbol{M}}$ are defined as

$$\boldsymbol{M} \equiv \boldsymbol{D}\{\text{diag}[\boldsymbol{D}^\top\boldsymbol{h}]\}^{-1}, \tag{3.26a}$$

$$\tilde{\boldsymbol{M}} \equiv \boldsymbol{D}\{\text{diag}[\boldsymbol{D}^\top(\text{diag}[\tilde{\boldsymbol{w}}])^{1-\sigma}\boldsymbol{h}]\}^{-1}. \tag{3.26b}$$

This leads to the following propositions.

Proposition 3.1 *The indirect utility* $\boldsymbol{v}(\boldsymbol{h}) \equiv [v_0(\boldsymbol{h}), v_1(\boldsymbol{h}), ..., v_{K-1}(\boldsymbol{h})]^\top$ *of each of the multi-region FO and Hm models is expressed as*[12]

$$\text{[FO model]} \quad \boldsymbol{v}(\boldsymbol{h}) = \kappa_{-}\boldsymbol{S}(\boldsymbol{h}) + \ln[\boldsymbol{w}(\boldsymbol{h})], \tag{3.27}$$

$$\text{[Hm model]} \quad \boldsymbol{v}(\boldsymbol{h}) = \kappa_{-}\tilde{\boldsymbol{S}}(\boldsymbol{h}) + \mu\ln[\tilde{\boldsymbol{w}}(\boldsymbol{h}) + \mathbf{1}] - (1-\mu)(\ln[\boldsymbol{h}] - \ln[\boldsymbol{A}]), \tag{3.28}$$

[12] We ignore the constant terms, which have no influence on the results in the following sections.

where $\kappa_- \equiv \mu/(\sigma-1)$, $\boldsymbol{A} \equiv [A_0, A_1, ..., A_{K-1}]^\top$, $\ln[\boldsymbol{w}] \equiv [\ln w_0, \ln w_1, ..., \ln w_{K-1}]^\top$,

$$\boldsymbol{S}(\boldsymbol{h}) \equiv \ln[\boldsymbol{D}^\top \boldsymbol{h}], \tag{3.29a}$$

$$\tilde{\boldsymbol{S}}(\boldsymbol{h}) \equiv \ln[\boldsymbol{D}^\top (\mathrm{diag}[\tilde{\boldsymbol{w}}])^{1-\sigma} \boldsymbol{h}], \tag{3.29b}$$

and the equilibrium wages $\boldsymbol{w}(\boldsymbol{h})$ *and* $\tilde{\boldsymbol{w}}(\boldsymbol{h})$ *are obtained from* (3.25).

Proposition 3.2 *For any* $\boldsymbol{h} \in \{[h_0, h_1, ..., h_{K-1}]^\top \mid \sum_i h_i = H, h_i \geq 0 \ \forall i\}$*, the multi-region FO and Hm models admit a unique short-run equilibrium.*

Proof see Appendix A.

3.3 Long-Run Equilibrium and Adjustment Dynamics

In the long run, the skilled workers are mobile across regions and will move to the region where their indirect utility is higher. The long-run equilibrium is defined as the spatial distribution of the mobile workers $\boldsymbol{h}$ that satisfies the following conditions:

$$\begin{cases} V^* - v_i(\boldsymbol{h}) = 0 & \text{if} \quad h_i > 0, \\ V^* - v_i(\boldsymbol{h}) \geq 0 & \text{if} \quad h_i = 0, \end{cases} \quad \forall i \tag{3.30a}$$

$$\sum_i h_i = H, \tag{3.30b}$$

where V^* denotes the equilibrium utility level. The condition (3.30a) means that a long-run equilibrium arises when no worker may get a higher utility level by moving to another region.

In order to define stability of long-run equilibrium, we assume the following adjustment process for the migration of skilled workers:

$$\dot{h}_i = F_i(\boldsymbol{h}) \equiv h_i\{v_i(\boldsymbol{h}) - \bar{v}(\boldsymbol{h})\} \quad \forall i, \tag{3.31}$$

where $\bar{v}(\boldsymbol{h})$ denotes the average utility level (i.e., $\bar{v}(\boldsymbol{h}) \equiv \sum_j (h_j/H) v_j(\boldsymbol{h})$), or equivalently written as

$$\dot{\boldsymbol{h}} = \boldsymbol{F}(\boldsymbol{h}) \equiv \mathrm{diag}[\boldsymbol{h}](\boldsymbol{v}(\boldsymbol{h}) - \bar{v}(\boldsymbol{h})\boldsymbol{1}). \tag{3.32}$$

This is the well-known replicator dynamic, which has been studied and routinely used in new economic geography and evolutionary game theory (e.g., Fujita et al. (1999), Weibull (1995), Sandholm (2010)).[13]

The dynamic (3.31) allows us to define stability of a long-run equilibrium $\boldsymbol{h}^*$ in the sense of local stability: the stability of the linearized system of (3.31) at $\boldsymbol{h}^*$. It

[13] It is noted that we can apply the proposed approach to the other dynamics. See Akamatsu et al. (2012) for the case of the perturbed best response dynamic, which is used in Tabuchi and Thisse (2002), Murata (2003) and Mossay (2003) to introduce the heterogeneity of the skilled worker.

is well known in dynamic system theory that the local stability of the equilibrium $\boldsymbol{h}^*$ is determined by examining the eigenvalues of the Jacobian matrix of the adjustment process $\boldsymbol{F}(\boldsymbol{h}) \equiv [F_0(\boldsymbol{h}), F_1(\boldsymbol{h}), ..., F_{K-1}(\boldsymbol{h})]^\top$ (See, for example, Hirsch and Smale (1974) and Hale and Koçak (1991))[14]:

$$\nabla \boldsymbol{F}(\boldsymbol{h}^*) = \boldsymbol{\psi}(\boldsymbol{h}^*)\nabla \boldsymbol{v}(\boldsymbol{h}^*) + \boldsymbol{J}(\boldsymbol{h}^*). \tag{3.33}$$

The matrices $\boldsymbol{\psi}(\boldsymbol{h})$ and $\boldsymbol{J}(\boldsymbol{h})$ in the right-hand side are represented as

$$\boldsymbol{\psi}(\boldsymbol{h}) = \text{diag}[\boldsymbol{h}](\boldsymbol{I} - H^{-1}\boldsymbol{E}\text{diag}[\boldsymbol{h}]), \tag{3.34}$$

$$\boldsymbol{J}(\boldsymbol{h}) = \text{diag}[\boldsymbol{v}(\boldsymbol{h}) - \bar{v}(\boldsymbol{h})\boldsymbol{1}] - H^{-1}\boldsymbol{h}\boldsymbol{v}(\boldsymbol{h})^\top, \tag{3.35}$$

and $\nabla \boldsymbol{v}(\boldsymbol{h})$ for the two models are given by

$$\text{[FO model]} \quad \nabla \boldsymbol{v}(\boldsymbol{h}) = \kappa_- \nabla \boldsymbol{S}(\boldsymbol{h}) + \{\text{diag}[\boldsymbol{w}(\boldsymbol{h})]\}^{-1}\nabla \boldsymbol{w}(\boldsymbol{h}), \tag{3.36}$$

$$\text{[Hm model]} \quad \nabla \boldsymbol{v}(\boldsymbol{h}) = \kappa_- \nabla \tilde{\boldsymbol{S}}(\boldsymbol{h}) + \mu\{\text{diag}[\tilde{\boldsymbol{w}}(\boldsymbol{h}) + \boldsymbol{1}]\}^{-1}\nabla \tilde{\boldsymbol{w}}(\boldsymbol{h}) - (1-\mu)\{\text{diag}[\boldsymbol{h}]\}^{-1}, \tag{3.37}$$

where $\boldsymbol{E}$ is a $K \times K$ matrix with all elements equal to 1, and $\nabla \boldsymbol{S}(\boldsymbol{h})$, $\nabla \boldsymbol{w}(\boldsymbol{h})$, $\nabla \tilde{\boldsymbol{S}}(\boldsymbol{h})$, and $\nabla \tilde{\boldsymbol{w}}(\boldsymbol{h})$ are the Jacobian matrices of $\boldsymbol{S}(\boldsymbol{h})$, $\boldsymbol{w}(\boldsymbol{h})$, $\tilde{\boldsymbol{S}}(\boldsymbol{h})$, and $\tilde{\boldsymbol{w}}(\boldsymbol{h})$, respectively.

4 Net Agglomeration Forces in a Racetrack Economy

4.1 Racetrack Economy and Spatial Discounting Matrix

Let us consider a *"racetrack economy,"* which represents the following geometry: 4 regions $\{0, 1, 2, 3\}$ are equidistantly located on the circumference of a circle with radius 1; the unskilled labor and the housing stocks are equally distributed across all regions (i.e., $l_i = l$, $A_i = A$ $\forall i$). Let $t(i, j)$ denote the distance between two regions i and j. We define the distance between the two regions as that measured by the minimum path length:

$$t(i, j) = \frac{2\pi}{4} m(i, j), \tag{4.1}$$

where $m(i, j) \equiv \min\{|i - j|, 4 - |i - j|\}$. The set $\{t(i, j), (i, j = 0, 1, 2, 3)\}$ of the distances determines the *spatial discounting matrix* $\boldsymbol{D}$ whose (i, j) element, d_{ij}, is given by

$$d_{ij} \equiv \exp[-(\sigma - 1)\tau t(i, j)]. \tag{4.2}$$

[14]The long-run equilibrium $\boldsymbol{h}^*$ in (3.30) is defined on the $(K-1)$-dimensional simplex $\{[h_0, h_1, ..., h_{K-1}]^\top | \sum_i h_i = H, h_i \geq 0 \ \forall i\}$. The extendibility of the Jacobian matrix for this simplex to the full K-dimension is presented in Sandholm (2010, Chap.3).

Defining the *spatial discount factor* (SDF) by

$$r \equiv \exp[-(\sigma - 1)\tau(2\pi/4)], \tag{4.3}$$

we can represent d_{ij} as $r^{m(i,j)}$. It follows from the definition that the SDF, r is a monotonically decreasing function of the transportation cost (technology) parameter τ, and hence the feasible range of the SDF (corresponding to $0 \leq \tau < +\infty$) is given by $(0, 1]$: $\tau = 0 \Leftrightarrow r = 1$, and $\tau \to +\infty \Leftrightarrow r \to 0$. Note here that the SDF yields the following expression for the SDM in a racetrack economy:

$$\boldsymbol{D} = \begin{bmatrix} 1 & r & r^2 & r \\ r & 1 & r & r^2 \\ r^2 & r & 1 & r \\ r & r^2 & r & 1 \end{bmatrix}. \tag{4.4}$$

As easily seen from this expression, the matrix $\boldsymbol{D}$ is *circulants*, which is constructed from the vector $\boldsymbol{d}_0 \equiv [1, r, r^2, r]$ (see Appendix C for the definition and properties of circulant matrices). This circulant property of the SDM plays a key role in the following analysis.

4.2 Stability, Eigenvalues, and Jacobian Matrices

The stability of equilibrium solutions for the FO and Hm models can be determined by examining the eigenvalues $\boldsymbol{g} \equiv [g_0, g_1, g_2, g_3]^\top$ of the Jacobian matrix of the adjustment process (3.31). Specifically, the equilibrium solution $\boldsymbol{h}$ satisfying (3.30a) and (3.30b) is asymptotically stable if all the eigenvalues of $\nabla \boldsymbol{F}(\boldsymbol{h})$ have negative real parts; otherwise, the solution is unstable (i.e., at least one eigenvalue of $\nabla \boldsymbol{F}(\boldsymbol{h})$ has a positive real part), and it moves in the direction of the corresponding eigenvector. The eigenvalues, if they are represented as functions of the key parameters of the FO model and the Hm model (e.g., transport technology parameter τ), further enable us to predict whether a particular agglomeration pattern (bifurcation) will occur with changes in the parameter values.

The eigenvalues $\boldsymbol{g}$ of the Jacobian matrix $\nabla \boldsymbol{F}(\boldsymbol{h})$ at an *arbitrary distribution* $\boldsymbol{h}$ of the skilled labor cannot be obtained without resorting to numerical techniques. It is, however, possible in some *symmetric distribution* $\bar{\boldsymbol{h}}$ to obtain analytical expressions for the eigenvalues $\boldsymbol{g}$ of the Jacobian matrix $\nabla \boldsymbol{F}(\bar{\boldsymbol{h}})$. The key tool for making this possible is a *circulant matrix*, which has several useful properties for the eigenvalue analysis. To take "Property 1" of a circulant in Appendix C for example, it implies that if $\nabla \boldsymbol{F}(\bar{\boldsymbol{h}})$ is a circulant, the eigenvalues $\boldsymbol{g}$ can be obtained by discrete Fourier transformation (DFT) of the first row vector $\boldsymbol{x}_0$ of $\nabla \boldsymbol{F}(\bar{\boldsymbol{h}})$:

$$\boldsymbol{g} = \boldsymbol{Z}\boldsymbol{x}_0^\top, \tag{4.5}$$

where $\boldsymbol{Z}$ is a 4×4 DFT matrix (i denotes the imaginary unit):

$$\boldsymbol{Z} \equiv \begin{bmatrix} 1 & 1 & 1 & 1 \\ 1 & \mathrm{i} & -1 & -\mathrm{i} \\ 1 & -1 & 1 & -1 \\ 1 & -\mathrm{i} & -1 & \mathrm{i} \end{bmatrix}, \tag{4.6}$$

and the k-th eigenvector is given by k-th row vector of $\boldsymbol{Z}$. Furthermore, "Property 2" assures us that $\nabla \boldsymbol{F}(\bar{\boldsymbol{h}})$ is indeed a circulant if the matrices in the right-hand side of (3.33) are all circulants.

A uniform distribution of skilled workers, $\bar{\boldsymbol{h}} \equiv [H/4, H/4, H/4, H/4]^\top$, which has intrinsic significance when examining the emergence of agglomeration, gives us a simple example for illustrating the use of the above properties of circulants. We first show below that the Jacobian matrix $\nabla \boldsymbol{F}(\bar{\boldsymbol{h}})$ at the uniform distribution $\bar{\boldsymbol{h}}$ is a circulant. This in turn allows us to obtain analytical expressions for the eigenvalues of $\nabla \boldsymbol{F}(\bar{\boldsymbol{h}})$, as will be shown in Section 4.3.

To show that $\nabla \boldsymbol{F}(\bar{\boldsymbol{h}})$ is a circulant, we examine each of the $\nabla \boldsymbol{v}(\bar{\boldsymbol{h}})$, $\boldsymbol{\psi}(\bar{\boldsymbol{h}})$, and $\boldsymbol{J}(\bar{\boldsymbol{h}})$ in turn. For the configuration $\bar{\boldsymbol{h}}$ in which $h \equiv H/4$, skilled workers are equally distributed in each region (i.e., $\bar{\boldsymbol{h}} \equiv [h, h, h, h]^\top$), the Jacobian matrix $\nabla \boldsymbol{v}(\bar{\boldsymbol{h}})$ of the indirect utility functions at $\bar{\boldsymbol{h}}$, which consists only of additions, multiplications, and their inverse of the circulant matrices $\bar{\boldsymbol{D}} \equiv \boldsymbol{D}/(1+r)^2$ and $\boldsymbol{I}$ as shown in Appendix B. It follows from this that $\nabla \boldsymbol{v}(\bar{\boldsymbol{h}})$ is a circulant. From (3.34) and (3.35), we have the Jacobian matrices $\boldsymbol{\psi}(\boldsymbol{h})$ and $\boldsymbol{J}(\boldsymbol{h})$ at $\bar{\boldsymbol{h}}$ as

$$\boldsymbol{\psi}(\bar{\boldsymbol{h}}) = h\left(\boldsymbol{I} - \frac{1}{4}\boldsymbol{E}\right) \tag{4.7}$$

$$\boldsymbol{J}(\bar{\boldsymbol{h}}) = -\frac{\bar{v}(\bar{\boldsymbol{h}})}{4}\boldsymbol{E} \tag{4.8}$$

This clearly shows that $\boldsymbol{\psi}(\bar{\boldsymbol{h}})$ and $\boldsymbol{J}(\bar{\boldsymbol{h}})$ are circulants because $\boldsymbol{I}$ and $\boldsymbol{E}$ are obviously circulants. Thus, matrices $\nabla \boldsymbol{v}(\bar{\boldsymbol{h}})$, $\boldsymbol{\psi}(\bar{\boldsymbol{h}})$, and $\boldsymbol{J}(\bar{\boldsymbol{h}})$ are circulants, and this leads to the conclusion that the Jacobian matrix of the adjustment process at the configuration $\bar{\boldsymbol{h}}$:

$$\nabla \boldsymbol{F}(\bar{\boldsymbol{h}}) = \boldsymbol{\psi}(\bar{\boldsymbol{h}}) \nabla \boldsymbol{v}(\bar{\boldsymbol{h}}) + \boldsymbol{J}(\bar{\boldsymbol{h}}) \tag{4.9}$$

is circulant.

4.3 Net Agglomeration Forces

The fact that matrices $\nabla \boldsymbol{v}(\bar{\boldsymbol{h}})$, $\boldsymbol{J}(\bar{\boldsymbol{h}})$, and $\boldsymbol{\psi}(\bar{\boldsymbol{h}})$ as well as $\nabla \boldsymbol{F}(\bar{\boldsymbol{h}})$ are circulants allows us to obtain the eigenvalues $\boldsymbol{g}$ of $\nabla \boldsymbol{F}(\bar{\boldsymbol{h}})$ by applying a similarity transformation based on the DFT matrix $\boldsymbol{Z}$. Specifically, the similarity transformation of both sides of (4.9) yields

$$\mathrm{diag}[\boldsymbol{g}] = h(\mathrm{diag}[\mathbf{1}] - \mathrm{diag}[\boldsymbol{\delta}])\mathrm{diag}[\boldsymbol{e}] - \bar{v}(\bar{\boldsymbol{h}})\mathrm{diag}[\boldsymbol{\delta}], \tag{4.10}$$

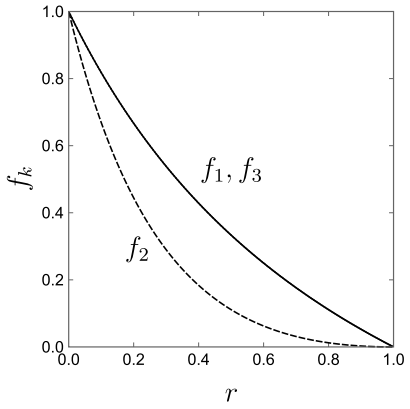

Figure 1: Eigenvalues f_k ($k = 1, 2, 3$) of $\bar{\boldsymbol{D}}$ as functions of the SDF r

where $\boldsymbol{\delta}$ and $\boldsymbol{e}$ are the eigenvalues of $(1/4)\boldsymbol{E}$ and $\nabla \boldsymbol{v}(\bar{\boldsymbol{h}})$, respectively. In a more concise form, this can be written as

$$\boldsymbol{g} = h[\mathbf{1} - \boldsymbol{\delta}] \cdot [\boldsymbol{e}] - \bar{v}(\bar{\boldsymbol{h}})\boldsymbol{\delta}, \tag{4.11}$$

where $[\boldsymbol{x}]\cdot[\boldsymbol{y}]$ denote the component-wise products of vectors $\boldsymbol{x}$ and $\boldsymbol{y}$. The two eigenvalues, $\boldsymbol{\delta}$ and $\boldsymbol{e}$, in the right-hand side of (4.10) and (4.11) can be easily obtained as follows. The former eigenvalues $\boldsymbol{\delta}$ are readily given by the DFT of the first row vector of $(1/4)\boldsymbol{E}$:

$$\boldsymbol{\delta} = \frac{1}{4}\boldsymbol{Z}\mathbf{1} = [1, 0, 0, 0]^\top. \tag{4.12}$$

As for the latter eigenvalues $\boldsymbol{e}$, note that $\nabla \boldsymbol{v}(\bar{\boldsymbol{h}})$ consists of additions, multiplications, and their inverse of the circulants $\bar{\boldsymbol{D}}$ and $\boldsymbol{I}$ (see (B.3) in Appendix B). This implies that the eigenvalues $\boldsymbol{e}$ can be represented as functions of the eigenvalues $\boldsymbol{f} \equiv [f_0, f_1, f_2, f_3]^\top$ of the spatial discounting matrix $\bar{\boldsymbol{D}}$. The eigenvalues $\boldsymbol{f}$, in turn, are obtained by the DFT of the first row vector $\boldsymbol{d}_0/d$ of $\bar{\boldsymbol{D}}$:

$$\boldsymbol{f} = \frac{1}{(1+r)^2}\boldsymbol{Z}\boldsymbol{d}_0^\top = [1, c(r), c(r)^2, c(r)]^\top, \tag{4.13}$$

where $c(r) \equiv (1-r)/(1+r) \in [0, 1)$. f_k ($k = 1, 2, 3$) is a monotonically decreasing function of r and $f_0 > f_1 = f_3 > f_2$ as illustrated in Figure 1. We then have the following proposition characterizing the eigenvalues and eigenvectors of the Jacobian matrix $\nabla \boldsymbol{F}(\bar{\boldsymbol{h}})$:

Proposition 4.1 *Consider a uniform distribution $\bar{\boldsymbol{h}} = [h, h, h, h]^\top$ of skilled workers in a racetrack economy with four regions. The Jacobian matrix $\nabla \boldsymbol{F}(\bar{\boldsymbol{h}})$ of the adjustment process* (3.31) *of the FO and Hm models at $\bar{\boldsymbol{h}}$ has the following eigenvector and the associated eigenvalues:*

1) *the k-th eigenvector ($k = 0, 1, 2, 3$) is given by the kth row vector, $\boldsymbol{z}_k$, of the discrete Fourier transformation (DFT) matrix $\boldsymbol{Z}$.*

2) *the k-th eigenvalue g_k of the FO model is given by a function of the k-th eigenvalue $f_k \in [0, 1)$*

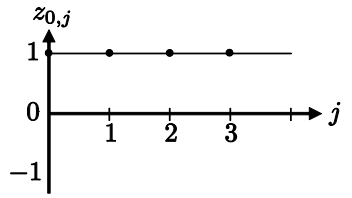

(a) $z_0 = [1, 1, 1, 1]$

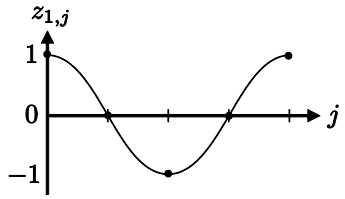

(b) $z_1 = [1, \mathrm{i}, -1, -\mathrm{i}]$

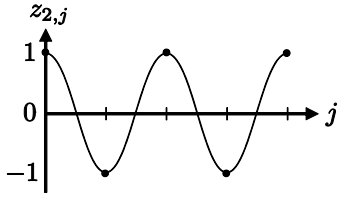

(c) $z_2 = [1, -1, 1, -1]$

Figure 2: Entry patterns of the eigenvectors

of the spatial discounting matrix $\bar{\boldsymbol{D}} \equiv \boldsymbol{D}/(1+r)^2$*:*

$$g_k = \frac{G(f_k)}{\phi(f_k)} \quad (k = 1, 2, 3), \qquad g_0 = -\bar{v}(\bar{\boldsymbol{h}}), \tag{4.14a}$$

$$G(x) \equiv bx - ax^2, \tag{4.14b}$$

where $\phi(x) \equiv 1 - \kappa x > 0$ *for* $x \in [0, 1)$*,* $a \equiv \kappa\kappa_- + 1$*,* $b \equiv \kappa + \kappa_-$*, and* f_k *is defined in* (4.13)*.*

3) the k-th eigenvalue g_k *of the Hm model is given by a function of* $f_k \in [0, 1)$*:*

$$g_k = \frac{\tilde{G}(f_k)}{\tilde{\phi}(f_k)} \quad (k = 1, 2, 3), \qquad g_0 = -\bar{v}(\bar{\boldsymbol{h}}), \tag{4.15a}$$

$$\tilde{G}(x) \equiv bx - \tilde{a}x^2 - (1 - \mu), \tag{4.15b}$$

where $\tilde{\phi}(x) \equiv 1 - \kappa x - (\kappa/\kappa_-)x^2 > 0$ *for* $x \in [0, 1)$ *and* $\tilde{a} \equiv \mu\kappa_- + \sigma^{-1} - (1 - \mu)$*.*

The eigenvectors $\{\boldsymbol{z}_k, (k = 0, 1, 2, 3)\}$ in the first part of Proposition 4.1 represent agglomeration patterns of skilled workers by the configuration pattern of the entries. For example, all entries of $\boldsymbol{z}_0 = [z_{0,0}, z_{0,1}, z_{0,2}, z_{0,3}]$ are equal to one, and the entry pattern of $\boldsymbol{z}_0 = [1, 1, 1, 1]$ corresponds to the state (configuration of skilled workers among four regions) in which skilled workers are uniformly distributed among four regions (see Figure 2a); $\boldsymbol{z}_2 = [1, -1, 1, -1]$ has the alternate sequence of 1 and -1 representing a duo-centric pattern in which skilled workers reside in two regions alternately (see Figure 2c); similarly, $\boldsymbol{z}_1$ and $\boldsymbol{z}_3$ correspond to a mono-centric pattern (see Figure 2b).

The eigenvalue g_k in the second and third parts of Proposition 4.1 can be interpreted as the strength of the "net agglomeration force" that leads the uniform distribution in the direction of the k-th agglomeration pattern (i.e., the k-th eigenvector). By the term the

"net agglomeration force," we mean the net effect of the "agglomeration force" minus "dispersion force." These forces correspond to the positive and negative terms of g_k (or functions $G(f_k)$ and $\tilde{G}(f_k)$).

The former (agglomeration) force is given by the term bx for both the FO and Hm models. As is clear from the derivation of the eigenvalues $\boldsymbol{g}$, this term stems from $\nabla \boldsymbol{S}$ and the positive term of $\nabla \boldsymbol{w}(\boldsymbol{h})$ (see (B.2) and (B.3) in Appendix B), each of which means the so-called "forward linkage" (or "price index effect") and "backward linkage" (or "demand effect"), respectively. This implies that this term represents the centripetal force induced by the increase in the variety of products that would be realized when the uniform distribution $\bar{\boldsymbol{h}}$ deviates to the agglomeration pattern $\boldsymbol{z}_k$.

The latter (dispersion) forces are somewhat different between the two models; they are given by the terms ax^2 and $\tilde{a}x^2 + (1 - \mu)$ for the FO and Hm models, respectively. The term ax^2 of the FO model, which stems from the negative term of $\nabla \boldsymbol{w}$, represents the centrifugal force due to increased market competition ("market crowding effect") in the agglomerated pattern $\boldsymbol{z}_k$. The term $\tilde{a}x^2 + (1 - \mu)$ of the Hm model represents the centrifugal force due to increased market competition and housing cost. Specifically, 1) the housing cost contributes only to the constant term $1 - \mu$ that is irrelevant to changes in f_k; and 2) the removal of immobile consumers in the Hm model reduces the coefficient of the quadratic term of f_k (i.e., the coefficient $\tilde{a}$ in the Hm model is always smaller than a in the FO model), which weakens the dispersion force.

Although the net agglomeration forces of the FO and Hm models share certain similarities (i.e., both are unimodal functions), they have subtle differences as can be seen from Figures 3a and 3b, the curve $\tilde{G}(f_k)$ for the Hm model is shifted to the right along the f_k axis in comparison with the curve $G(f_k)$ for the FO model. This is due to the following differences in the dispersion forces mentioned above: 1) the introduction of the housing cost in the Hm model adds the constant term of the dispersion force, which shifts the crossing point x^*_- of G to the crossing point $\tilde{x}^*_-$ of $\tilde{G}$; and 2) the removal of immobile consumers in the Hm model shifts the crossing point x^*_+ of G to the crossing point $\tilde{x}^*_+$ of $\tilde{G}$. These shifts result in the reversal of the signs of $\tilde{G}(f_k)$ and $G(f_k)$ at the boundaries of f_k (i.e., $f_k = 0$ and 1). As shown in the following sections, this fact causes significant differences in the evolutionary processes of agglomeration patterns in the two models. Specifically, $\tilde{G}(1) > 0$ implies that the Hm model does not satisfy the so-called "no black-hole condition" in NEG, which in turn implies that no poly-centric agglomerations should occur in stable equilibria. Therefore, we can say that every model satisfying the no black-hole condition exhibits essentially the same evolutionary processes of agglomeration patterns as the FO model. To elucidate this, we shall compare the bifurcation process (caused by changes in transportation cost) of the FO and Hm models, each of which, in turn, is analyzed in sections 5 and 6, respectively.

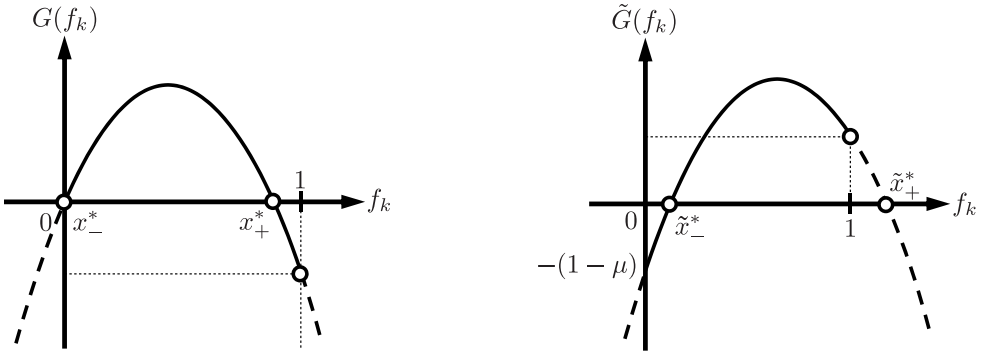

(a) FO model (b) Hm model

Figure 3: Net agglomeration forces as functions of f_k

5 Theoretical Prediction of Agglomeration Patterns of the FO model

5.1 Emergence of Agglomeration

We first analyze the multi-region FO model. In order for bifurcation from the uniform equilibrium distribution $\bar{\boldsymbol{h}} = [h, h, h, h]^\top$ to occur with the changes in the SDF r (or the transportation cost τ), either of the eigenvalues $g_1 (= g_3)$ and g_2 must change signs. Since the eigenvalues g_k $(k = 1, 2, 3)$ are given by $G(f_k)/\phi(f_k)$ where $\phi(x) > 0$ for $x \in [0, 1)$, the sign changes imply that the quadratic equation with respect to f_k:

$$G(x) = bx - ax^2 = 0, \tag{5.1}$$

should have real solutions in the interval $[0, 1)$ that is the possible range of the eigenvalue f_k (see (4.13) and Figure 1). This leads us to the following proposition:

Proposition 5.1 *In the FO model, a bifurcation from a uniform equilibrium distribution* $\bar{\boldsymbol{h}} = [h, h, h, h]^\top$ *occurs with the changes in the SDF r if and only if the parameters satisfy*

$$b < a, \tag{5.2}$$

where $a \equiv \kappa\kappa_- + 1$, $b \equiv \kappa + \kappa_-$, $\kappa \equiv \mu/\sigma$ *and* $\kappa_- \equiv \mu/(\sigma - 1)$.

The inequality (5.2) corresponds to the "no black-hole" condition, which is well known in literature that deals with the two-regional NEG model. For the cases when parameters of the FO model do not satisfy this condition, the eigenvalues g_k $(k = 1, 2, 3)$ are positive even when the SDF is zero (i.e., transportation cost τ is very high), which implies that the uniform distribution $\bar{\boldsymbol{h}}$ cannot be a stable equilibrium.

In the following analyses, we assume that the parameters (σ, μ) of the FO model satisfy (5.2). We then have two real solutions for the quadratic equation $G(f_k) = 0$ with

respect to f_k:

$$x_+^* \equiv \frac{b}{a} \quad \text{and} \quad x_-^* \equiv 0. \tag{5.3}$$

Each of the solutions $x_\pm^*$ means a critical value ("break point") at which a bifurcation from the flat earth equilibrium $\bar{\boldsymbol{h}}$ occurs when we regard the eigenvalue f_k as a bifurcation parameter. This fact can be easily seen in Figure 3a: the flat earth equilibrium $\bar{\boldsymbol{h}}$ is stable (i.e., $G(f_k)$ is negative) for high values of f_k in the range $(x_+^*, 1]$, and hence, when we consider the process of decreasing the value of f_k from $f_k = 1$, the bifurcation from $\bar{\boldsymbol{h}}$ occurs (i.e, sign of $G(f_k)$ changes) at $f_k = x_+^*$.

Since we are interested in the emergence of agglomeration (bifurcation) that would arise with changes in transportation costs, we shall take the SDF r (rather than f_k) as a bifurcation parameter, and *consider the process of increasing the SDF starting from* $r = 0$ at which the uniform distribution is a unique equilibrium. Let us recall here that each of the eigenvalues $\{f_k(r)\}$ is a monotonically decreasing function of the SDF (see (4.13) and Figure 1). This implies that the flat earth equilibrium $\bar{\boldsymbol{h}}$ is stable for low values of r corresponding to the range $(x_+^*, 1]$ of $f_k(r)$, and that the eigenvalue $f_k(r)$ crosses the critical value x_+^* in the process of increasing the SDF.

In this process, we see from (4.13) that the eigenvalue $f_2(r)$ first reaches the critical value x_+^* before $f_1(r)$ does, since $f_2(r)$ is always smaller than $f_1(r)$:

$$f_1(r) \equiv c(r) > f_2(r) \equiv c(r)^2 \qquad \forall r \in (0, 1]. \tag{5.4}$$

Thus, we can conclude that the first bifurcation occurs when the SDF first reaches the critical value r_+^* that satisfies

$$x_+^* = f_2(r_+^*) \equiv c(r_+^*)^2. \tag{5.5}$$

To be more specific, the critical value r_+^* of the SDF is given by

$$r_+^* = \frac{1 - \sqrt{x_+^*}}{1 + \sqrt{x_+^*}}. \tag{5.6}$$

It is worth noting that (5.6) implicitly provides information on the changes in r_+^* with the changes in values of the FO model parameters (σ, μ) since x_+^* is explicitly represented as a function of the FO model parameters in (5.3).

The fact that the eigenvalue $f_2(r)$ first crosses the critical value x_+^* also enables us to identify the associated agglomeration pattern that emerges at the first bifurcation. Let us recall here that the equilibrium solution moves in the direction of the eigenvector whose associated eigenvalue first hits the critical value. As stated in Proposition 4.1, this direction is the second eigenvector $\boldsymbol{z}_2 = [1, -1, 1, -1]$. Therefore, the pattern of

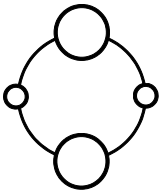

Figure 4: Agglomeration pattern of the FO model that emerges from the uniform distribution

agglomeration that first emerges is

$$\boldsymbol{h} = \bar{\boldsymbol{h}} + \delta \boldsymbol{z}_2^\top = [h+\delta, h-\delta, h+\delta, h-\delta]^\top \quad (0 \leq \delta \leq h), \tag{5.7}$$

in which skilled workers agglomerate in two alternate regions (Figure 4).[15] Thus, we can characterize the bifurcation from the uniform distribution as follows.

Proposition 5.2 *Suppose that the conditions of* (5.2) *in Proposition 5.1 are satisfied for the FO model, and that the uniform distribution* $\bar{\boldsymbol{h}} = [h, h, h, h]^\top$ *of skilled workers is a stable equilibrium at some value of the SDF* $r\,(< r_+^*)$*. Starting from this state, we consider the process where the value of the SDF continuously increases (i.e., the transportation cost* τ *decreases).*

1) *The net agglomeration force (i.e., the eigenvalue)* g_k *for each agglomeration pattern (i.e., the eigenvector)* $\boldsymbol{z}_k$ *increases as the SDF increases, and the uniform distribution becomes unstable (i.e., agglomeration emerges) at the break point* $r = r_+^*$ *given by* (5.3) *and* (5.6) *(see Figure 5).*

2) *The critical value* r_+^* *for the bifurcation decreases, as a) the expenditure share on industrial varieties is larger (i.e.,* μ *is large), and b) the elasticity of substitution between two varieties is smaller (i.e.,* σ *is small).*

3) *The pattern of agglomeration that first emerges is* $\boldsymbol{h} = [h+\delta, h-\delta, h+\delta, h-\delta]^\top$ $(0 \leq \delta \leq h)$*, in which skilled workers agglomerate alternately in two regions (see Figure 4).*

A few remarks are in order about the bifurcation at the latter critical value x_-^*. Since the critical value x_-^* is obtained as (5.3), we have

$$r_k(x_-^*) = r_k(0) = 1 \qquad (k = 1, 2, 3). \tag{5.8}$$

This implies that the net agglomeration forces $\boldsymbol{g}$ are always positive for the interval $[r_+^*, 1)$ of the SDF. This fact is illustrated in Figure 5, where the horizontal axis denotes the SDF r, and the solid curve denotes the eigenvalue g_1 as a function of r, while the dashed curve denotes the eigenvalue g_2. Both curves are unimodal functions whose values

[15] It is known in the group-theoretic bifurcation theory (Ikeda and Murota, 2010; Ikeda et al., 2012a) that the symmetry of an equilibrium is preserved until undergoing a bifurcation. Therefore, the agglomeration pattern $\bar{\boldsymbol{h}} + \delta \boldsymbol{z}_2^\top$ $(0 \leq \delta \leq 1)$ that emerges at the first bifurcation must be an equilibrium of the FO model.

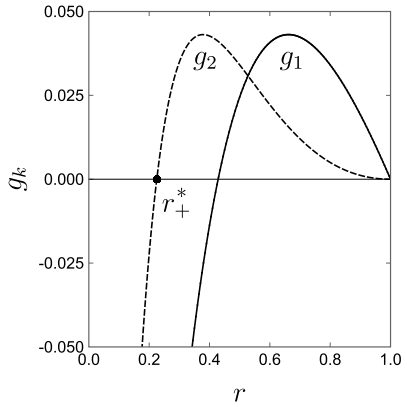

Figure 5: Eigenvalues g_1 and g_2 of the FO model as functions of the spatial discounting factor ($\sigma = 3.0, \mu = 0.5$)

reach zero at $r = 1$. Therefore, the critical value of the SDF at which the bifurcation from agglomeration equilibrium to the flat earth equilibrium occurs is

$$r_-^* = 1. \tag{5.9}$$

That is, no matter how large the SDF is, agglomeration never breaks down, except for the maximum limit at $r = 1$.

5.2 Evolution of Agglomeration

In conventional FO model (and other NEG models) with two regions, increases in the SDF (or decreases in transportation cost τ) lead to the occurrence of a bifurcation from the uniform distribution $\bar{\boldsymbol{h}}$ to a mono-centric agglomeration. In the FO model with four (or more) regions, the first bifurcation shown in Section 5.1 does not directly branch to the mono-centric pattern; instead, further bifurcations (leading to a more concentrated pattern) can repeatedly occur.

5.2.1 Evolution to a Duo-centric Pattern $\boldsymbol{h}^*$ — Sustain Point for $\boldsymbol{h}^*$

For the FO model, the deviation δ from the uniform distribution $\bar{\boldsymbol{h}}$ monotonically increases with the increases in the SDF after the first bifurcation. Shortly after the increases in the SDF from the break point $r = r_+^*$, this leads to a duo-centric pattern, $\boldsymbol{h}^* = [2h, 0, 2h, 0]^\top$, where only the two alternate regions are equally populated by skilled workers. The fact that the duo-centric pattern $\boldsymbol{h}^*$ may exist as an equilibrium solution of the FO model can be confirmed by examining the "sustain point" for $\boldsymbol{h}^*$. The sustain point is the value of the SDF above which the equilibrium condition for $\boldsymbol{h}^*$

$$v_0(\boldsymbol{h}^*) = v_2(\boldsymbol{h}^*) = \max_k \{v_k(\boldsymbol{h}^*)\} \tag{5.10}$$

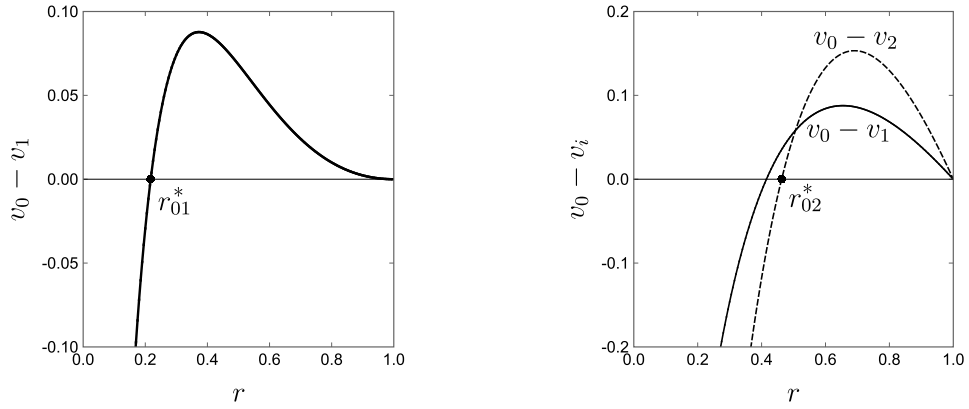

(a) The sustain point for $\boldsymbol{h}^*$

(b) The sustain point for $\boldsymbol{h}^{**}$

Figure 6: Sustainable regions for $\boldsymbol{h}^* = [2h, 0, 2h, 0]^\top$ and $\boldsymbol{h}^{**} = [4h, 0, 0, 0]^\top$ ($\sigma = 3.0$, $\mu = 0.5$)

is satisfied. As shown in Appendix D, the condition of (5.10) indeed holds for any r larger than r^*_{01}, which is the sustain point for $\boldsymbol{h}^*$. This is illustrated in Figure 6a, where the horizontal axis denotes the SDF r, and the curve represents the utility difference $v_0(\boldsymbol{h}^*) - v_1(\boldsymbol{h}^*)$ as a function of r. As seen in this figure, $v_0(\boldsymbol{h}^*) - v_1(\boldsymbol{h}^*)$ is positive for any r larger than r^*_{01} (the sustain point), which means that the duo-centric pattern $\boldsymbol{h}^*$ continues to be an equilibrium for the range of the SDF above the sustain point.

5.2.2 Bifurcation from the Duo-centric Pattern — Break Point at h^*

After the emergence of the duo-centric pattern $\boldsymbol{h}^* = [2h, 0, 2h, 0]^\top$, further increases in the SDF (above the sustain point $r = r^*_{01}$) can lead to further bifurcations (i.e., $\boldsymbol{h}^*$ become unstable). To investigate such a possibility, we need to obtain the eigenvectors and the associated eigenvalues for the Jacobian matrix of the adjustment process at $\boldsymbol{h}^*$:

$$\nabla \boldsymbol{F}(\boldsymbol{h}^*) = \boldsymbol{J}(\boldsymbol{h}^*) + \boldsymbol{\psi}(\boldsymbol{h}^*)\nabla \boldsymbol{v}(\boldsymbol{h}^*). \tag{5.11}$$

A possible difficulty we encounter in obtaining the eigenvalues is that the Jacobian $\nabla \boldsymbol{F}(\boldsymbol{h}^*)$ at $\boldsymbol{h}^*$ is no longer a circulant matrix, unlike the Jacobian $\nabla \boldsymbol{F}(\bar{\boldsymbol{h}})$ at $\bar{\boldsymbol{h}}$. This is due to the loss of symmetry in the configuration of skilled workers (see Figure 7), which leads to the fact that $\boldsymbol{J}(\boldsymbol{h}^*)$, $\boldsymbol{\psi}(\boldsymbol{h}^*)$, and $\nabla \boldsymbol{v}(\boldsymbol{h}^*)$ are not circulants. However, as it turns out, it is still possible to find a closed-form expression for the eigenvalues of $\nabla \boldsymbol{F}(\boldsymbol{h}^*)$ by using the fact that the duo-centric pattern $\boldsymbol{h}^*$ has partial symmetry and the submatrices of $\boldsymbol{J}(\boldsymbol{h}^*)$, $\boldsymbol{\psi}(\boldsymbol{h}^*)$, and $\nabla \boldsymbol{v}(\boldsymbol{h}^*)$ are circulants (see Lemma E.1).

In order to exploit the symmetry remaining in the duo-centric pattern $\boldsymbol{h}^*$, we begin by dividing set $C = \{0, 1, 2, 3\}$ of regions into two subsets: subset $C_0 = \{0, 2\}$ of regions with skilled workers, and subset $C_1 = \{1, 3\}$ of regions without skilled workers. Corresponding to this division of the set of regions, we consider the following permutation σ of set

uniform distribution duo-centric pattern

Figure 7: Symmetry of the two configurations $\bar{\boldsymbol{h}} = [h, h, h, h]^\top$ and $\boldsymbol{h}^* = [2h, 0, 2h, 0]^\top$

$C = \{0, 1, 2, 3\}$,

$$\sigma(0) = 0, \quad \sigma(1) = 2, \quad \sigma(2) = 1, \quad \sigma(3) = 3, \tag{5.12}$$

such that the first half elements $\{\sigma(0), \sigma(1)\}$ and the second half elements $\{\sigma(2), \sigma(3)\}$ of set $C^P = \{\sigma(0), \sigma(1), \sigma(2), \sigma(3)\}$ correspond to subsets C_0 and C_1, respectively. For this permutation, we then define the associated permutation matrix $\boldsymbol{P}$:

$$\boldsymbol{P} \equiv \begin{bmatrix} 1 & 0 & 0 & 0 \\ 0 & 0 & 1 & 0 \\ 0 & 1 & 0 & 0 \\ 0 & 0 & 0 & 1 \end{bmatrix}. \tag{5.13}$$

It can be readily verified that, for a 4×4 matrix $\boldsymbol{A}$ whose (i, j) element is denoted as a_{ij}, $\boldsymbol{PAP}^\top$ yields a matrix whose (i, j) element is $a_{\sigma(i)\sigma(j)}$, and that $\boldsymbol{PP}^\top = \boldsymbol{P}^\top\boldsymbol{P} = \boldsymbol{I}$; that is, the similarity transformation $\boldsymbol{PAP}^\top$ offers a consistent renumbering of the rows and columns of $\boldsymbol{A}$ by the permutation σ.

The permutation σ (or the similarity transformation based on the permutation matrix $\boldsymbol{P}$) constitutes a "new coordinate system" for analyzing the Jacobian matrix of the adjustment process. Under the new coordinate system, the SDM $\boldsymbol{D}$ can be represented as

$$\boldsymbol{PDP}^\top = \left[\begin{array}{c:c} \boldsymbol{D}^{(0)} & \boldsymbol{D}^{(1)} \\ \hdashline \boldsymbol{D}^{(1)} & \boldsymbol{D}^{(0)} \end{array}\right], \tag{5.14}$$

where each of the submatrices $\boldsymbol{D}^{(0)}$ and $\boldsymbol{D}^{(1)}$ is a 2×2 circulant matrix generated from a vector $\boldsymbol{d}_0^{(0)} \equiv [1, r^2]$ and $\boldsymbol{d}_0^{(1)} \equiv [r, r]$, respectively. Similarly, the Jacobian matrix $\nabla\boldsymbol{F}(\boldsymbol{h}^*)$ of the adjustment process is transformed into

$$\boldsymbol{P}\nabla\boldsymbol{F}(\boldsymbol{h}^*)\boldsymbol{P}^\top = \boldsymbol{PJ}(\boldsymbol{h}^*)\boldsymbol{P}^\top + \left\{\boldsymbol{P}\psi(\boldsymbol{h}^*)\boldsymbol{P}^\top\right\}\left\{\boldsymbol{P}\nabla\boldsymbol{v}(\boldsymbol{h}^*)\boldsymbol{P}^\top\right\}, \tag{5.15}$$

where the Jacobian matrices on the right-hand side are respectively defined by

$$\boldsymbol{P}\nabla\boldsymbol{v}(\boldsymbol{h}^*)\boldsymbol{P}^\top = \frac{1}{2h}\left[\begin{array}{c:c} \boldsymbol{V}^{(00)} & \boldsymbol{V}^{(01)} \\ \hdashline \boldsymbol{V}^{(10)} & \boldsymbol{V}^{(11)} \end{array}\right], \tag{5.16a}$$

$$\boldsymbol{P}\boldsymbol{J}(\boldsymbol{h}^*)\boldsymbol{P}^\top = \left[\begin{array}{c|c} -(1/2)\bar{v}(\boldsymbol{h}^*)\boldsymbol{E} & -(1/2)v_1(\boldsymbol{h}^*)\boldsymbol{E} \\ \hline \boldsymbol{0} & (v_1(\boldsymbol{h}^*) - \bar{v}(\boldsymbol{h}^*))\boldsymbol{I} \end{array}\right], \tag{5.16b}$$

$$\boldsymbol{P}\boldsymbol{\psi}(\boldsymbol{h}^*)\boldsymbol{P}^\top = 2h\left[\begin{array}{c|c} \boldsymbol{I} - (1/2)\boldsymbol{E} & \boldsymbol{0} \\ \hline \boldsymbol{0} & \boldsymbol{0} \end{array}\right], \tag{5.16c}$$

and submatrices $\boldsymbol{V}^{(ij)}$ and $\boldsymbol{J}^{(ij)}$ $(i, j = 0, 1)$ are 2×2 matrices.

For these Jacobian matrices under the new coordinate system, we can show (Lemma E.1) that all of the submatrices $\boldsymbol{V}^{(ij)}$ are circulants. This fact allows us to conclude (Lemma E.2) that knowing only the eigenvalues $\boldsymbol{e}^{(00)}$ of the submatrix $\boldsymbol{V}^{(00)} = \{dv_i/dh_j, (i, j \in C_0)\}$ is sufficient to obtain the eigenvalues $\boldsymbol{g}^*$ of the Jacobian $\nabla \boldsymbol{F}(\boldsymbol{h}^*)$. Furthermore, it can be readily shown that the submatrix $\boldsymbol{V}^{(00)}$ is a circulant consisting only of submatrices $\boldsymbol{D}^{(0)}$ and $\boldsymbol{D}^{(1)}$ of the SDM $\boldsymbol{D}$ (these are also circulants). This implies that we can obtain analytical expressions for the eigenvalues $\boldsymbol{e}^{(00)}$. These considerations lead to the following lemma:

Lemma 5.1 *The Jacobian matrix $\nabla \boldsymbol{F}(\boldsymbol{h}^*)$ of the adjustment process* (3.31) *of the FO model at $\boldsymbol{h}^*$ has the following eigenvector and the associated eigenvalues:*

1) *The k-th eigenvector $(k = 0, 1, 2, 3)$ is given by the k-th row vector, $\boldsymbol{z}_k^*$, of the discrete Fourier transformation (DFT) matrix*

$$\boldsymbol{Z}^* \equiv \boldsymbol{P}^\top \mathrm{diag}[\boldsymbol{Z}_{[2]}, \boldsymbol{Z}_{[2]}]\boldsymbol{P}, \quad \text{where} \quad \boldsymbol{Z}_2 \equiv \begin{bmatrix} 1 & 1 \\ 1 & -1 \end{bmatrix}. \tag{5.17}$$

2) *The eigenvalues $\{g_k^*, (k = 0, 1, 2, 3)\}$ are given by $g_0^* = -\bar{v}(\boldsymbol{h}^*)$, $g_k^* = v_1(\boldsymbol{h}^*) - \bar{v}(\boldsymbol{h}^*)$ $(k = 1, 3)$, and*

$$g_2^* = \frac{\hat{G}(c(r^2))}{\phi(c(r^2))}, \tag{5.18}$$

$$\hat{G}(x) \equiv bx - a^* x^2 \tag{5.19}$$

where $\phi(x) \equiv 1 - \kappa x > 0$, $c(r^2) \equiv (1 - r^2)/(1 + r^2)$, $b \equiv \kappa + \kappa_-$ and $a^* \equiv \kappa\kappa_- + (\kappa + 1)/2$.

Proof see Appendix E.

The eigenvalues $\boldsymbol{g}^*$ obtained in Lemma 5.1 allow us to determine the critical value ("break point") at which a bifurcation from the duo-centric pattern $\boldsymbol{h}^* = [2h, 0, 2h, 0]^\top$ to a more concentrated pattern occurs. In a similar manner to the discussion for the first bifurcation from the uniform distribution $\bar{\boldsymbol{h}} = [h, h, h, h]^\top$, we see that the second bifurcation from the duo-centric pattern $\boldsymbol{h}^*$ occurs when the eigenvalue $g_2^*(x)$ changes signs. Since $g_2^*(x)$ is given by (5.18), the critical values of $x \equiv c(r^2)$ at which the eigenvalue changes signs are the solutions of the quadratic equation $\hat{G}(x) = 0$. Hence, the critical

values (the two solutions of (5.19)) are given by

$$x_+^{**} = \frac{b}{a^*} = \frac{2(\kappa + \kappa_-)}{2\kappa\kappa_- + \kappa + 1} \quad \text{and} \quad x_-^{**} = 0. \tag{5.20}$$

Note here that $x \equiv c(r^2)$ is a monotonically decreasing function of the SDF and its interval is $[0, 1)$. This implies that, in the course of increasing the SDF, x only crosses x_+^{**}. Therefore, the second bifurcation occurs when the SDF reaches the critical value r_+^{**} that satisfies $x_+^{**} = c(\{r_+^{**}\}^2)$. That is, the critical value of the second bifurcation in terms of the SDF is given by

$$r_+^{**} = \sqrt{\frac{1 - x_+^{**}}{1 + x_+^{**}}}. \tag{5.21}$$

We can also identify the associated agglomeration pattern that emerges at this bifurcation. The movement away from $\boldsymbol{h}^*$ at this bifurcation is the second eigenvector $\boldsymbol{z}_2^* = [1, 0, -1, 0]$. Accordingly, the emerging spatial configuration is given by

$$\boldsymbol{h} = \boldsymbol{h}^* + \delta\{\boldsymbol{z}_2^*\}^\top = [2h + \delta, 0, 2h - \delta, 0]^\top \qquad (0 \le \delta \le 2h). \tag{5.22}$$

Thus, the properties of the second bifurcation can be summarized as follows:

Proposition 5.3 *Suppose that the SDF r is larger than the sustain point r_{01}^* of the duo-centric pattern $\boldsymbol{h}^* = [2h, 0, 2h, 0]^\top$ and $\boldsymbol{h}^*$ is a stable equilibrium for the FO model. With the increases in the SDF, the duo-centric pattern $\boldsymbol{h}^*$ become unstable at the second break point $r = r_+^{**}$ given by* (5.20) *and* (5.21)*, and then a more concentrated pattern $\boldsymbol{h} = [2h + \delta, 0, 2h - \delta, 0]^\top$ $(0 \le \delta \le 2h)$ emerges.*

5.2.3 Evolution to a Mono-centric Pattern h^{**} — Sustain Point for h^{**}

After the second bifurcation, the deviation δ from the duo-centric pattern $\boldsymbol{h}^* = [2h, 0, 2h, 0]^\top$ increases monotonically with the increase in the SDF, which leads to a mono-centric pattern, $\boldsymbol{h}^{**} = [4h, 0, 0, 0]^\top$. This fact can be confirmed by examining the sustain point for the mono-centric pattern. As shown in Appendix D, the equilibrium condition for $\boldsymbol{h}^{**}$,

$$v_0(\boldsymbol{h}^{**}) = \max_k \{v_k(\boldsymbol{h}^{**})\} \tag{5.23}$$

is satisfied for any $r > r_{02}^{**}$ (the critical value), which is the sustain point for $\boldsymbol{h}^{**}$. This is illustrated in Figure 6b, where the horizontal axis denotes the SDF, and the solid and dashed curves are the utility differences $v_0(\boldsymbol{h}^{**}) - v_1(\boldsymbol{h}^{**})$ and $v_0(\boldsymbol{h}^{**}) - v_2(\boldsymbol{h}^{**})$ as a function of r, respectively. As seen in this figure, $v_0(\boldsymbol{h}^{**})$ provides the largest utility for any $r > r_{02}^{**}$ (the sustain point), which means that the mono-centric pattern $\boldsymbol{h}^{**}$ continues to be an equilibrium for the range $1 > r > r_{02}^{**}$.

The results obtained up to this point are summarized in the schematic representation

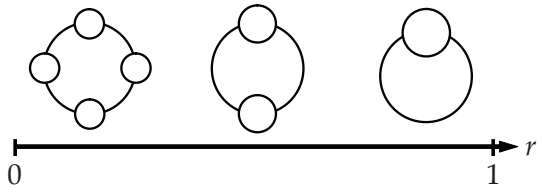

Figure 8: A series of agglomeration patterns that emerge in the course of increasing the SDF: spatial period-doubling cascade

shown in Figure 8. This clearly shows the occurrence of the spatial period-doubling cascade.

6 Theoretical Prediction of Agglomeration Patterns of the Hm Model

6.1 Emergence of Agglomeration

We next investigate the evolution of the agglomeration pattern in the Hm model by the approach described in Section 5. In order for bifurcation from the uniform equilibrium distribution $\bar{\boldsymbol{h}} = [h, h, h, h]^\top$ to occur with the changes in the SDF r (or the transportation cost τ), either of the eigenvalues $g_1 (= g_3)$ and g_2 must change signs. Since the eigenvalues g_k $(k = 1, 2, 3)$ are given by $\tilde{G}(f_k)/\tilde{\phi}(f_k)$ where $\tilde{\phi}(x) > 0$ for $x \in [0, 1)$, the sign changes mean that the following quadratic equation with respect to f_k,

$$\tilde{G}(x) = bx - \tilde{a}x^2 - (1 - \mu) = 0, \tag{6.1}$$

should have real solutions. That is,

$$\Theta \equiv b^2 - 4\tilde{a}(1 - \mu) > 0 \tag{6.2}$$

should be satisfied. Moreover, either of the solutions, $\tilde{x}^*_\pm \equiv (b \pm \sqrt{\Theta})/2\tilde{a}$, must lie in the interval $[0, 1)$, which is the possible range of the eigenvalue f_k. Note here that, under the condition (6.2) for the existence of real solutions, this requirement cannot be satisfied for one of the solutions $\tilde{x}^*_+$ (see Figure 3b), and hence, the requirement is reduced to the only condition for the other solution $\tilde{x}^*_-$,

$$\tilde{x}^*_- \equiv \frac{b - \sqrt{\Theta}}{2\tilde{a}} < 1. \tag{6.3}$$

Thus, we see that inequalities (6.2) and (6.3) need to be satisfied for the occurrence of a bifurcation from a uniform distribution. This leads to the following proposition.

Proposition 6.1 *In the Hm model, a bifurcation from a uniform equilibrium distribution* $\bar{\boldsymbol{h}}$

occurs with the changes in the SDF r if and only if the parameters satisfy,

$$(1-\mu)\sigma < 1. \tag{6.4}$$

This proposition shows that for any agglomeration to occur, the increasing returns, $1/\sigma$, must dominate the dispersion force, $1-\mu$, generated by the demand for immobile land.

In the following analysis, we assume that the parameters (σ, μ) of the Hm model satisfy (6.4). The solution $\tilde{x}^*_-$ for the quadratic equation $\tilde{G}(f_k) = 0$ with respect to f_k means that the critical value at which a bifurcation from the flat earth equilibrium $\bar{\boldsymbol{h}}$ occurs when we regard the eigenvalue f_k as a bifurcation parameter. This can be easily seen from Figure 3b where the flat earth equilibrium $\bar{\boldsymbol{h}}$ is stable (i.e., $\tilde{G}(f_k)$ is negative) for low values of f_k in the range $[0, \tilde{x}^*_-)$, and hence, when we consider the process of increasing the value of f_k from $f_k = 0$, the bifurcation from $\bar{\boldsymbol{h}}$ occurs (i.e, sign of $\tilde{G}(f_k)$ changes) at $f_k = \tilde{x}^*_-$.

In fact, Redding and Sturm (2008) calibrated the spatial distribution of population in Germany in 1939 under the assumption of $(1-\mu)\sigma > 1$ (instead of (6.4)) which admits only the (unique) complete dispersion, i.e., flat earth equilibrium, in the present setting. Although the "complete dispersion" is not necessarily a uniform distribution if the regions are asymmetrically placed as in Redding and Sturm (2008), it should be noted that this parameter range does *not* admit the formation of any agglomeration based on the positive externalities assumed in the model. In their paper, the primary determinant of the spatial distribution of population was the *unobserved non-traded amenity* which is the "housing stock, A_i," for each region i in the present model. Here, this exogenous city-specific factor was not obtained from the data, but was determined to account for the deviation of the actual population distribution among cities from the complete dispersion. Consequently, nearly 90% of city size variation was explained by the *unobserved* city-fixed effect (refer to footnote 2).

In order to compare the evolutionary process of the spatial agglomeration in the Hm model with that in the FO model, we shall take the SDF r (rather than f_k) as a bifurcation parameter. In contrast to the analysis of the FO model, *we consider the process of decreasing the SDF starting from* $r = 1$. This reflects the fact that, unlike the FO model, the flat earth equilibrium $\bar{\boldsymbol{h}}$ is stable for high values of r corresponding to the range $[0, \tilde{x}^*_-)$ of $f_k(r)$, and the eigenvalue $f_k(r)$ crosses the critical value $\tilde{x}^*_-$ in the process of decreasing the SDF starting from $r = 1$.

In this process, unlike the process of increasing r for the analysis of the FO model, we see from (4.13) that, the eigenvalue $f_1(r) = f_3(r)$ first reaches the critical value $\tilde{x}^*_-$ before $f_2(r)$ does, since $f_1(r)$ is always larger than $f_2(r)$. Therefore, the first bifurcation occurs when the SDF reaches the critical value $\tilde{r}^*$ that satisfies

$$\tilde{x}^*_- = f_1(\tilde{r}^*) \equiv c(\tilde{r}^*). \tag{6.5}$$

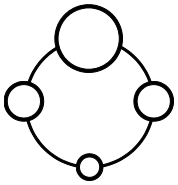

Figure 9: Agglomeration pattern of the Hm model that emerges from the uniform distribution

To be more specific, the critical value $\tilde{r}^*$ of the SDF is given by

$$\tilde{r}^* = \frac{1 - \tilde{x}^*_-}{1 + \tilde{x}^*_-}. \tag{6.6}$$

The fact that the eigenvalue $f_1(r)$ first crosses the critical value $\tilde{x}^*$ implies that the equilibrium solution moves in the direction of the first (or third) eigenvector $\boldsymbol{z}_1 = [1, 0, -1, 0]$. Therefore, the pattern of agglomeration that first emerges is

$$\boldsymbol{h} = \bar{\boldsymbol{h}} + \delta \boldsymbol{z}_1^\top = [h + \delta, h, h - \delta, h]^\top \tag{6.7}$$

in which skilled workers agglomerate in a single region (Figure 9). Thus, we can characterize the bifurcation from the uniform distribution as follows.

Proposition 6.2 *Suppose that the conditions of* (6.4) *in Proposition 6.1 are satisfied for the Hm model, and that the uniform distribution* $\bar{\boldsymbol{h}} = [h, h, h, h]^\top$ *of skilled workers is a stable equilibrium at some value of the SDF* r $(> \tilde{r}^*)$*. Starting from this state, we consider the process where the value of the SDF continuously decreases (i.e., the transportation cost* τ *increases).*

1) *The net agglomeration force (i.e., the eigenvalue)* g_k *for each agglomeration pattern (i.e., the eigenvector)* $\boldsymbol{z}_k$ *increases as the SDF decreases, and the uniform distribution becomes unstable (i.e., agglomeration emerges) at the break point* $r = \tilde{r}^*$ *given by* (6.3) *and* (6.6) *(see Figure 10).*

2) *The critical value* $\tilde{r}$ *for the bifurcation increases, as a) the expenditure share on industrial varieties is larger (i.e.,* μ *is large), b) the elasticity of substitution between two varieties is smaller (i.e.,* σ *is small).*

3) *The pattern of agglomeration that first emerges is* $\boldsymbol{h} = [h + \delta, h, h - \delta, h]^\top$*, in which skilled workers agglomerate toward a region (see Figure 9), i.e., the spatial distribution of skilled workers is a unimodal distribution over the regions.*

By comparing Propositions 5.2, 5.3, and 6.2, we see that the agglomeration properties of the FO model and the Hm model are significantly different. The FO model exhibits a cascade of bifurcation in the course of decreasing the transportation costs: a uniform distribution of mobile factors on four symmetric regions first bifurcates to a duo-centric agglomeration pattern, and further decreases as the transportation costs

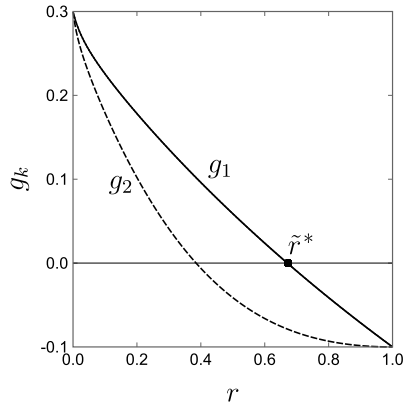

Figure 10: Eigenvalues g_1 and g_2 of the Hm model as functions of the spatial discounting factor ($\sigma = 2.0$, $\mu = 0.8$)

trigger the occurrence of a second bifurcation, which in turn leads to the formation of a mono-centric agglomeration. In contrast, the Hm model undergoes only a single bifurcation through the course of increasing the transportation costs: the uniform distribution directly branches to a unimodal distribution.

This difference in agglomeration processes is essentially a consequence of the difference between the two possible bifurcations from the flat earth equilibrium: one at the right critical point x^*_+ and the other at the left critical point x^*_-, where each of the two critical points is the value of f_k at which the uni-modal function $G(f_k)$ (or $\tilde{G}(f_k)$) of the net agglomeration force changes signs. Let us recall here the two curves, $G(f_k)$ and $\tilde{G}(f_k)$, of the net agglomeration forces depicted in Figure 3 where the curve $\tilde{G}(f_k)$ for the Hm model is shifted to the right in comparison with the curve $G(f_k)$ for the FO model. This leads to the fact that, in the FO model, the bifurcation from the flat earth equilibrium occurs only at the right critical point x^*_+ while, in the Hm model, it occurs only at the left critical point x^*_-. Since the eigenvectors (i.e., the direction of changes in the distribution of mobile factors) activated by these two bifurcations are different, the resultant spatial patterns of agglomeration for the two models also are different. Thus, we see that the agglomeration process in the Hm model is not simply a "reversal" of that in the FO model, but a qualitatively different one.

6.2 Instability of the Duo-centric Pattern

In this section, we show that poly-centric agglomeration patterns do not emerge in a stable equilibrium for the Hm model. In the context of the four-region economy, it amounts to showing that a duo-centric pattern cannot occur in a stable equilibrium. Specifically, we clarify here that the duo-centric pattern (Figure 4), which emerges in the FO model, *never* emerges in the Hm model.

In order to assess the stability of the duo-centric pattern $\boldsymbol{h}_2 = [h_0, h_1, h_0, h_1]^\top$ ($h_0 > h_1$), we need to check the sign of the eigenvalues of $\nabla \boldsymbol{F}(\boldsymbol{h}_2)$. Because $\nabla \boldsymbol{F}(\boldsymbol{h}_2)$ is symmetric,

the Rayleigh quotient $R(\nabla \boldsymbol{F}(\boldsymbol{h}_2))$ of $\nabla \boldsymbol{F}(\boldsymbol{h}_2)$ must lie between the largest eigenvalue $g_{\max}$ and the smallest eigenvalue $g_{\min}$ of $\nabla \boldsymbol{F}(\boldsymbol{h}_2)$:

$$R(\nabla \boldsymbol{F}(\boldsymbol{h}_2), \boldsymbol{x}) = \frac{\boldsymbol{x}^\top \nabla \boldsymbol{F}(\boldsymbol{h}_2)\boldsymbol{x}}{\boldsymbol{x}^\top \boldsymbol{x}} \in [g_{\min}, g_{\max}], \tag{6.8}$$

where $\boldsymbol{x}$ is a nonzero 4×1 vector. Furthermore, $R(\nabla \boldsymbol{F}(\boldsymbol{h}_2), \boldsymbol{x})$ has the following property:

Lemma 6.1 *Suppose that $\boldsymbol{h}_2$ is an equilibrium of the Hm model. Then, for any r less than $\tilde{r}^*$,*

$$R(\nabla \boldsymbol{F}(\boldsymbol{h}_2), \boldsymbol{z}_1^\top) > 0. \tag{6.9}$$

Proof See Appendix F

This lemma shows that the largest eigenvalue $g_{\max}$ of $\nabla \boldsymbol{F}(\boldsymbol{h}_2)$ must be positive when the uniform distribution is unstable. This leads to the following proposition.

Proposition 6.3 *In the Hm model, the duo-centric pattern $\boldsymbol{h}_2$ cannot be a stable equilibrium if the uniform distribution $\bar{\boldsymbol{h}}$ is unstable.*

A key implication of Proposition 6.3 is that when the complete dispersion ceases to be a stable equilibrium, poly-centric agglomeration patterns do not emerge as stable equilibria in the multi-region extension of the Hm model.[16] Thus, this model by itself cannot replicate poly-centric agglomeration patterns observed in reality. Although the dispersion force considered in the Hm model is relevant in reality, it becomes useful only when it is combined with other dispersion forces as in the FO model. While most variants of Krugman (1991) directly assume the presence of dispersed consumers, it is also possible to make this dispersion endogenous. For instance, Fujita and Krugman (1995) considered that the production of the A-sector requires labor and land as inputs, and assumed that workers employed in this sector live where they work, which in turn resulted in the endogenous dispersion of consumers.

7 Numerical Examples

This section describes numerical examples of the evolutionary process of agglomeration patterns in order to illustrate the theoretical results shown in Sections 5 and 6. The parameter values in these cases are identical with those in Figures 5 and 10 (i.e., $\sigma = 3.0, \mu = 0.5$ for the FO model and $\sigma = 2.0, \mu = 0.8$ for the Hm model). For the computation of these examples, we employ the algorithm developed by Ikeda et al. (2012a), which applies the computational bifurcation theory to the multi-region NEG model. This algorithm allows us to obtain a complete picture of the evolutionary process of the agglomeration patterns including the transition processes. The results of the numerical

[16] This implies that the results of Redding and Sturm (2008), which uses the multi-region Hm model for the empirical analysis, can be significantly changed if the FO model is employed.

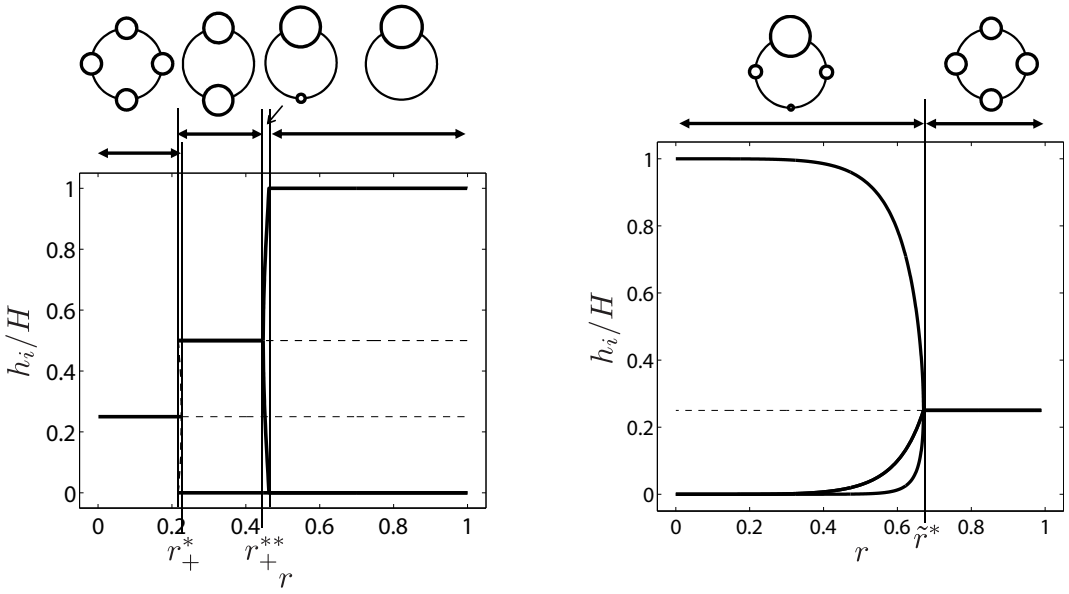

(a) FO model (b) Hm model

Figure 11: Evolution of the agglomeration pattern

analysis are shown in Figure 11, in which the horizontal axis denotes the SDF r and the curves represent the fraction h_i/H of the skilled workers in each region.

FO Model: Figure 11a shows the evolutionary process of the agglomeration patterns of the FO model in the course of increasing r. First, the spatial pattern is the uniform distribution until r is smaller than the break point r_+^*. When r reaches r_+^*, the first bifurcation occurs and the duo-centric pattern emerges. As r keeps increasing, the second bifurcation occurs at r_+^{**}, and this increase in r leads to the mono-centric pattern. These results are consistent with Propositions 5.2 and 5.3. In addition, it is worth noting that, though the first pitchfork bifurcation is supercritical (i.e., a catastrophic agglomeration occurs), the second pitchfork bifurcation is subcritical (i.e., a smooth agglomeration occurs).

Hm Model: The evolutionary process of the Hm model, which is illustrated in Figure 11b, is significantly different from (i). The agglomeration pattern of this model directly evolves from a uniform distribution toward the unimodal distribution as r decreases. This result clearly shows that the evolutionary process of the Hm model is not the opposite of that of the FO model.

8 Concluding Remarks

Using NEG models, this study has shown that an extension of a two-region model with agglomeration externalities to a multi-region one (with more than two regions) does not necessarily admit the possibility of poly-centric agglomeration patterns. Thus, to

replicate the observed poly-centric agglomeration patterns in reality, one needs to be careful in selecting an appropriate model. More specifically, we compared two types of NEG models by Forslid and Ottaviano (2003) and Helpman (1998). It has been shown that the former model exhibits multi-stage bifurcations in response to decreases in transportation costs where a uniform distribution of mobile factors on four symmetric regions first bifurcates to a duo-centric agglomeration pattern, which continues to be stable for a range of transportation costs; further decreases in transportation costs trigger the second bifurcation resulting in the formation of a mono-centric agglomeration. In contrast, the latter model undergoes only a single bifurcation through the course of increasing transportation costs and the uniform distribution directly branches to a mono-centric pattern. Furthermore, it has been formally proved that a duo-centric pattern never emerges in the latter model.

Methodologically, we demonstrated that the spatial discounting matrix (SDM) encapsulates the essential information required for analyzing the multi-region NEG models. Specifically, in order to understand the spatial concentration-dispersion patterns that may emerge in the NEG models, it suffices: a) to obtain the eigenvalues of the SDM; and b) to represent the Jacobian matrix of the indirect utility as a function of the SDM. It should be emphasized that this fact holds for a wide variety of models that deal with endogenous agglomerations of economic activities. Indeed, the same procedure as that of this paper can be readily applied to other types of agglomeration models other than NEG models, such as self-organizing urban structure models with endogenous CBD formation (Takayama and Akamatsu, 2011; Osawa et al., 2015).

Although we focused on the possibility of poly-centric agglomerations in the context of *a homogeneous circular space*, asymmetries of location space could be important determinants of the spatial pattern of mobile agents in reality. Besides heterogeneous regional endowments whose relevance has been extensively discussed recently (e.g., Allen and Arkolakis, 2014; Caliendo et al., 2015; Desmet and Rossi-Hansberg, 2013), the presence of edges in the location space could often explain the formation of major cities, such that New York and Los Angeles at the coasts became substantially larger than the inland cities in the US. Although analytical investigations become suddenly tough once under these asymmetries, Ikeda et al. (2015) showed that the FO model exhibits a striking resemblance in the agglomeration characteristics between the long narrow economy and the racetrack economy by utilizing computational bifurcation theory suggested by Ikeda et al. (2012a).

Finally, it should be kept in mind that the models which admit poly-centric agglomerations are still not enough as candidate models to replicate the agglomeration patterns in reality. In the case of NEG models studied in this paper, all individual agglomerations in stable poly-centric equilibria for the FO model have equal size. In fact, in the absence of *exogenous location-specific factors*, this is a common behavior among the NEG models with a single type of differentiated goods where the substitutability between each pair of differentiated goods is symmetric (e.g., Krugman, 1991; Forslid and Ottaviano, 2003;

Pflüger, 2004; Behrens and Murata, 2007). In the context of NEG models, one way to endogenously generate a large size diversity among agglomerations is to introduce multiple differentiated industries as in Fujita et al. (1999, Chap.11) and Tabuchi and Thisse (2011). While Tabuchi and Thisse (2011) made an initial step in this direction, the development of more general approach is left for future research.[17]

[17]Refer to Hsu (2012) for an alternative model to NEG introducing multiple differentiated industries.

Appendix

A Proof of Proposition 3.2

For the proof of Proposition 3.2, it suffices to show that the uniqueness of the price index (3.23a) and the wage (3.25a) of the multi-region FO and Hm models. Thus, we prove the uniqueness of these variables of two models in turn.

FO model

(1) From (3.23a), we can confirm that the price index $\boldsymbol{\rho}$ is uniquely determined.

(2) It follows from (3.25a) that the wage $\boldsymbol{w}$ is uniquely determined if the matrices $\mathrm{diag}[\boldsymbol{D}^\top \boldsymbol{h}]$ and $\{\boldsymbol{I} - (\mu/\sigma)\boldsymbol{M}\mathrm{diag}[\boldsymbol{h}]\}$ are invertible. The former is true since it is readily verified that

$$\det|\mathrm{diag}[\boldsymbol{D}^\top \boldsymbol{h}]| > 0. \tag{A.1}$$

The latter can be proved if the matrix $\{\boldsymbol{I} - (\mu/\sigma)\boldsymbol{M}\mathrm{diag}[\boldsymbol{h}]\}$ satisfies Hawkins-Simon condition (Hawkins and Simon, 1949). From Theorem 6.1 of Nikaido (1968, p.90), this condition is equivalent to the following condition: there is a positive vector $\boldsymbol{x}$ such that

$$\left[\boldsymbol{I} - \frac{\mu}{\sigma}\boldsymbol{M}\mathrm{diag}[\boldsymbol{h}]\right]\boldsymbol{x} > \boldsymbol{0}. \tag{A.2}$$

Substituting $\boldsymbol{x} = \boldsymbol{D}\boldsymbol{h} (> \boldsymbol{0})$ into the left hand side of (A.2), we have

$$\left[\boldsymbol{I} - \frac{\mu}{\sigma}\boldsymbol{M}\mathrm{diag}[\boldsymbol{h}]\right]\boldsymbol{D}\boldsymbol{h} = \left(1 - \frac{\mu}{\sigma}\right)\boldsymbol{D}\boldsymbol{h}. \tag{A.3}$$

Since σ is larger than μ in the FO model, (A.2) is always satisfied. Therefore, the wage of the FO model is uniquely determined.

Hm model

(1) From (3.23b), the price index $\boldsymbol{\rho}$ is uniquely determined if the equilibrium wage $\tilde{\boldsymbol{w}}$ is unique.

(2) The wage equations (3.25b) are equivalent to the following problem:

$$\boldsymbol{\Psi}(\tilde{\boldsymbol{w}}) = \boldsymbol{0}, \tag{A.4a}$$

$$\begin{aligned}\boldsymbol{\Psi}(\tilde{\boldsymbol{w}}) &= [\Psi_i(\boldsymbol{w})] \\ &= \left[w_i h_i - \mu \sum_j \frac{d_{ij} w_i^{1-\sigma} h_i}{\sum_k d_{kj} w_k^{1-\sigma} h_k}(w_j + 1)h_j\right].\end{aligned} \tag{A.4b}$$

If there exists a short-run equilibrium wage $\tilde{\boldsymbol{w}}^*$ (i.e., $\boldsymbol{\Psi}(\tilde{\boldsymbol{w}}^*) = \boldsymbol{0}$), $\tilde{\boldsymbol{w}}^*$ is a solution of the following nonlinear complementarity problem (NCP)

$$\tilde{\boldsymbol{w}} \cdot \boldsymbol{\Psi}(\tilde{\boldsymbol{w}}) = 0, \quad \tilde{\boldsymbol{w}} \geq \boldsymbol{0}, \quad \boldsymbol{\Psi}(\tilde{\boldsymbol{w}}) \geq \boldsymbol{0}. \tag{A.5}$$

It is known that, if $\nabla\boldsymbol{\Psi}(\tilde{\boldsymbol{w}}) = [\partial\Psi_i/\partial w_j]$ is a P matrix for all $\tilde{\boldsymbol{w}} \in \mathbb{R}_+$, NCP (A.5) has at most one solution.[18] Furthermore, $\nabla\boldsymbol{\Psi}(\tilde{\boldsymbol{w}})$ is a P matrix for all $\tilde{\boldsymbol{w}} \in \mathbb{R}_+$ if $\nabla\boldsymbol{\Psi}(\tilde{\boldsymbol{w}})$ satisfies the following condition (see Cottle et al., 2009):

$$\max_i w_i[\nabla\boldsymbol{\Psi}(\tilde{\boldsymbol{w}})\tilde{\boldsymbol{w}}]_i > 0 \quad \forall\tilde{\boldsymbol{w}} \in \mathbb{R}_+. \tag{A.6}$$

Because $[\nabla\boldsymbol{\Psi}(\tilde{\boldsymbol{w}})\tilde{\boldsymbol{w}}]_i$ is given by

$$[\nabla\boldsymbol{\Psi}(\tilde{\boldsymbol{w}})\tilde{\boldsymbol{w}}]_i = h_i w_i - \mu\sum_j \frac{d_{ij}w_i^{1-\sigma}h_i}{\sum_k d_{kj}w_k^{1-\sigma}h_k}w_j h_j \tag{A.7}$$

and $\sum_i[\nabla\boldsymbol{\Psi}(\tilde{\boldsymbol{w}})\tilde{\boldsymbol{w}}]_i = (1-\mu)\sum_i h_i w_i > 0$, we have $[\nabla\boldsymbol{\Psi}(\tilde{\boldsymbol{w}})\tilde{\boldsymbol{w}}]_i > 0$ and $w_i > 0$ for $i = \arg\max_i[\nabla\boldsymbol{\Psi}(\tilde{\boldsymbol{w}})\tilde{\boldsymbol{w}}]_i$. This shows that $\nabla\boldsymbol{\Psi}(\tilde{\boldsymbol{w}})$ is a P matrix for all $\tilde{\boldsymbol{w}} \in \mathbb{R}_+$, and thus NCP (A.5) has at most one solution. This indicates that the short-run equilibrium wage $\tilde{\boldsymbol{w}}^*$ is uniquely determined if there exists $\tilde{\boldsymbol{w}}^*$. Therefore, we next prove the existence of $\tilde{\boldsymbol{w}}^*$.

The wage equations is also equivalent to the following fixed point problem:

find $\tilde{\boldsymbol{w}} \in \mathcal{W}$ such that $w_i = \Phi_i(\tilde{\boldsymbol{w}})\ \forall i$,

where $\Phi_i(\tilde{\boldsymbol{w}}) = \mu\sum_j \frac{d_{ij}w_i^{1-\sigma}}{\sum_k d_{kj}w_k^{1-\sigma}h_k}(w_j+1)h_j$, $\mathcal{W} = \left\{\tilde{\boldsymbol{w}} \;\middle|\; \sum_i w_i h_i = \frac{\mu}{1-\mu}H,\ \tilde{\boldsymbol{w}} \geq \mathbf{0}\right\}$,

because $\sum_i \Psi_i(\tilde{\boldsymbol{w}}) = 0$ gives $\sum_i w_i h_i = H\mu/(1-\mu)$. It follows from this, $\Phi_i(\tilde{\boldsymbol{w}}) \in \mathcal{W}$, and Brouwer's fixed point theorem that there exists at least one short-run equilibrium wage $\tilde{\boldsymbol{w}}$. Therefore, the short-run equilibrium wage and price index are uniquely determined.

B Jacobian Matrices of the Indirect Utility of the FO Model and the Hm Model

The Jacobian matrix, $\nabla\boldsymbol{v}$, in the right-hand side of (3.33) of the FO model and the Hm model are expressed as (3.36) and (3.37), respectively. The matrices $\nabla\boldsymbol{S}(\boldsymbol{h})$ and $\nabla\boldsymbol{w}(\boldsymbol{h})$ in (3.36) are given by

$$\nabla\boldsymbol{S}(\boldsymbol{h}) = \boldsymbol{M}^\top, \tag{B.1a}$$

$$\nabla\boldsymbol{w}(\boldsymbol{h}) = \kappa\{\boldsymbol{I} - \kappa\boldsymbol{M}\mathrm{diag}[\boldsymbol{h}]\}^{-1}\{\boldsymbol{M}\mathrm{diag}[\boldsymbol{w}(\boldsymbol{h})] - \boldsymbol{M}\boldsymbol{Y}(\boldsymbol{h})\boldsymbol{M}^\top\}, \tag{B.1b}$$

$$\boldsymbol{Y}(\boldsymbol{h}) \equiv \mathrm{diag}[\boldsymbol{w}(\boldsymbol{h})]\mathrm{diag}[\boldsymbol{h}] + l\boldsymbol{I}. \tag{B.1c}$$

The matrices $\nabla\tilde{\boldsymbol{S}}(\boldsymbol{h})$ and $\nabla\tilde{\boldsymbol{w}}(\boldsymbol{h})$ in (3.37) are expressed as

$$\nabla\tilde{\boldsymbol{S}}(\boldsymbol{h}) = \tilde{\boldsymbol{M}}^\top(\mathrm{diag}[\tilde{\boldsymbol{w}}])^{1-\sigma} - (\sigma-1)\tilde{\boldsymbol{M}}^\top\mathrm{diag}[\boldsymbol{h}](\mathrm{diag}[\tilde{\boldsymbol{w}}(\boldsymbol{h})])^{-\sigma}\nabla\tilde{\boldsymbol{w}}(\boldsymbol{h}), \tag{B.2a}$$

[18] For the proof, see, e.g., Facchinei and Pang (2003)

$$\nabla\tilde{\boldsymbol{w}}(\boldsymbol{h}) = -\left(\frac{\partial \boldsymbol{W}(\tilde{\boldsymbol{w}},\boldsymbol{h})}{\partial \tilde{\boldsymbol{w}}}\right)^{-1} \frac{\partial \boldsymbol{W}(\tilde{\boldsymbol{w}},\boldsymbol{h})}{\partial \boldsymbol{h}}, \tag{B.2b}$$

$$\boldsymbol{W}(\tilde{\boldsymbol{w}},\boldsymbol{h}) \equiv \mu\tilde{\boldsymbol{M}}\mathrm{diag}[\boldsymbol{h}](\tilde{\boldsymbol{w}}+\boldsymbol{1}) - (\mathrm{diag}[\tilde{\boldsymbol{w}}])^{\sigma}\boldsymbol{1}, \tag{B.2c}$$

$$\begin{aligned}\frac{\partial \boldsymbol{W}(\tilde{\boldsymbol{w}},\boldsymbol{h})}{\partial \tilde{\boldsymbol{w}}} = {} & \mu\tilde{\boldsymbol{M}}\mathrm{diag}[\boldsymbol{h}]\{\boldsymbol{I} + (\sigma-1)\mathrm{diag}[\tilde{\boldsymbol{w}}+\boldsymbol{1}]\tilde{\boldsymbol{M}}^{\top}(\mathrm{diag}[\tilde{\boldsymbol{w}}])^{-\sigma}\mathrm{diag}[\boldsymbol{h}]\} \\ & - \sigma(\mathrm{diag}[\tilde{\boldsymbol{w}}])^{\sigma-1},\end{aligned} \tag{B.2d}$$

$$\frac{\partial \boldsymbol{W}(\tilde{\boldsymbol{w}},\boldsymbol{h})}{\partial \boldsymbol{h}} = \mu\tilde{\boldsymbol{M}}\mathrm{diag}[\tilde{\boldsymbol{w}}+\boldsymbol{1}]\{\boldsymbol{I} - \mathrm{diag}[\boldsymbol{h}]\tilde{\boldsymbol{M}}^{\top}(\mathrm{diag}[\tilde{\boldsymbol{w}}])^{1-\sigma}\}. \tag{B.2e}$$

For the configuration $\bar{\boldsymbol{h}} \equiv [h,h,h,h]^{\top}$, the definitions of $\boldsymbol{M}$ and $\tilde{\boldsymbol{M}}$ in (3.26) yield $\boldsymbol{M}(\bar{\boldsymbol{h}}) = (hd)^{-1}\boldsymbol{D}$, $\tilde{\boldsymbol{M}}(\bar{\boldsymbol{h}}) = (h\tilde{w}^{1-\sigma}d)^{-1}\boldsymbol{D}$, where $d \equiv \boldsymbol{d}_0 \cdot \boldsymbol{1} = (1+r)^2$ and $\tilde{w} \equiv \mu/(1-\mu)$, and hence the Jacobian matrix of the indirect utility functions at $\bar{\boldsymbol{h}}$ reduces to

$$\text{[FO model]} \quad \nabla\boldsymbol{v}(\bar{\boldsymbol{h}}) = \frac{1}{h}\left\{\kappa_{-}\bar{\boldsymbol{D}} + [\boldsymbol{I} - \kappa\bar{\boldsymbol{D}}]^{-1}\bar{\boldsymbol{D}}[\kappa\boldsymbol{I} - \bar{\boldsymbol{D}}]\right\}, \tag{B.3a}$$

$$\text{[Hm model]}\ \nabla\boldsymbol{v}(\bar{\boldsymbol{h}}) = \frac{1}{h}\left\{\kappa_{-}\bar{\boldsymbol{D}} + \kappa(\mu\boldsymbol{I} - \bar{\boldsymbol{D}})\left[\boldsymbol{I} - \kappa\bar{\boldsymbol{D}} - \frac{\kappa}{\kappa_{-}}\bar{\boldsymbol{D}}^2\right]^{-1}\bar{\boldsymbol{D}}(\boldsymbol{I} - \bar{\boldsymbol{D}}) - (1-\mu)\boldsymbol{I}\right\}, \tag{B.3b}$$

where $\bar{\boldsymbol{D}} \equiv \boldsymbol{D}/d$.

C Properties of Circulant Matrices

A circulant $\boldsymbol{C}$ is defined as a square matrix of the form

$$\boldsymbol{C} \equiv \begin{bmatrix} c_0 & c_1 & c_2 & \cdots & c_{K-2} & c_{K-1} \\ c_{K-1} & c_0 & c_1 & c_2 & \cdots & c_{K-2} \\ \vdots & \vdots & & & & \vdots \\ c_2 & c_3 & \cdots & c_{K-1} & c_0 & c_1 \\ c_1 & c_2 & \cdots & c_{K-2} & c_{K-1} & c_0 \end{bmatrix}. \tag{C.1}$$

The elements of each row of $\boldsymbol{C}$ are identical to those of the previous row, but are moved one position to the right and wrapped around. The whole circulant is evidently determined by the first row vector $\boldsymbol{c} = [c_0, c_1, \cdots, c_{K-1}]$. Circulant matrices satisfy the following two well-known properties[19].

Property 1 Every circulant matrix $\boldsymbol{C}$ is diagonalized by the following similarity transformation:

$$\boldsymbol{Z}^{*}\boldsymbol{C}\boldsymbol{Z} = \mathrm{diag}[\boldsymbol{\lambda}], \tag{C.2}$$

where $\boldsymbol{Z}$ is the DFT matrix whose (j,k) entry is given by $\omega^{jk} = \exp[\mathrm{i}(2\pi jk/K)]$, $\mathrm{i} \equiv$

[19]For the proofs of these properties, see, for example, Horn and Johnson (2013), Gray (2006)

$\sqrt{-1}$; $\boldsymbol{\lambda} \equiv [\lambda_0, \lambda_1, \cdots, \lambda_{K-1}]^\top$, and $\boldsymbol{Z}^*$ denotes the conjugate transpose of $\boldsymbol{Z}$. The k-th eigenvalues and the eigenvectors of $\boldsymbol{C}$ are therefore λ_k and the k-th row of the DFT matrix $\boldsymbol{Z}$, respectively. Furthermore, $\boldsymbol{\lambda}$ is directly given by the DFT of the first row vector $\boldsymbol{c}$ of $\boldsymbol{C}$: $\boldsymbol{\lambda} = \boldsymbol{Z}\boldsymbol{c}^\top$.

Property 2 If $\boldsymbol{C}_1$ and $\boldsymbol{C}_2$ are circulant matrices, the sum $\boldsymbol{C}_1 + \boldsymbol{C}_2$ and the product $\boldsymbol{C}_1\boldsymbol{C}_2$ are circulants. Also, if $\boldsymbol{C}_1$ is nonsingular, its inverse $\boldsymbol{C}_1^{-1}$ is a circulant.

D Sustain Points for $\boldsymbol{h}^* = [2h, 0, 2h, 0]^\top$ and $\boldsymbol{h}^{**} = [4h, 0, 0, 0]^\top$

We will show the derivation of sustain points for $\boldsymbol{h}^* = [2h, 0, 2h, 0]^\top$ and $\boldsymbol{h}^{**} = [4h, 0, 0, 0]^\top$, in turn.

(1) For the duo-centric pattern $\boldsymbol{h}^* = [2h, 0, 2h, 0]^\top$, we can easily obtain the indirect utility for each region by substituting $\boldsymbol{h} = \boldsymbol{h}^*$ into (3.27):

$$v_i(\boldsymbol{h}^*) = \begin{cases} \kappa_- \ln[2hd_{(0)}] + \ln\left[\dfrac{\kappa}{1-\kappa}\dfrac{l}{h}\right] & \text{if} \quad i = 0, 2 \\ \kappa_- \ln[2hd_{(1)}] + \ln\left[\dfrac{\kappa}{1-\kappa}\dfrac{l}{2h}\left((1+\kappa)\dfrac{d_{(1)}}{d_{(0)}} + (1-\kappa)\dfrac{d_{(0)}}{d_{(1)}}\right)\right] & \text{if} \quad i = 1, 3 \end{cases} \tag{D.1}$$

where $d_{(0)} \equiv 1 + r^2$ and $d_{(1)} \equiv 2r$. To obtain the sustain point for $\boldsymbol{h}^*$, we represent the utility difference between the "core" regions and the "periphery" regions as a function of the SDF:

$$\begin{aligned} v_{01}(r) &\equiv v_0(\boldsymbol{h}^*) - v_1(\boldsymbol{h}^*) \\ &= \kappa_- \ln\left[\frac{d_{(0)}}{d_{(1)}}\right] - \ln\left[\frac{1}{2}\left((1+\kappa)\frac{d_{(1)}}{d_{(0)}} + (1-\kappa)\frac{d_{(0)}}{d_{(1)}}\right)\right] \end{aligned} \tag{D.2}$$

By inspecting the function $v_{01}(r)$, we see that it takes zero value at $r = 1$ and $r = r_{01}^* > 0$ (i.e., the equation $v_{01}(r) = 0$ has two positive solutions 1 and r_{01}^*) and that

$$v_{01}(r) \begin{cases} < 0 & \text{for} \quad 0 < r < r_{01}^*, \\ \geq 0 & \text{for} \quad r_{01}^* \leq r < 1. \end{cases} \tag{D.3}$$

This means that the equilibrium condition for $\boldsymbol{h}^*$, $v_0(\boldsymbol{h}^*) = v_2(\boldsymbol{h}^*) = \max_k\{v_k(\boldsymbol{h}^*)\}$, is satisfied for any r larger than r_{01}^*; that is, $r = r_{01}^*$ is the sustain point for $\boldsymbol{h}^*$.

(2) The sustain point for the mono-centric pattern $\boldsymbol{h}^{**} = [4h, 0, 0, 0]^\top$ can be obtained in a

similar manner. The indirect utility at $\boldsymbol{h}^{**}$ is given by

$$v_i(\boldsymbol{h}^{**}) = \begin{cases} \kappa_- \ln[4h] + \ln\left[\dfrac{\kappa}{1-\kappa}\dfrac{l}{h}\right] & \text{if} \quad i = 0, \\ \kappa_- \ln[4rh] + \ln\left[\dfrac{\kappa}{1-\kappa}\dfrac{l}{2h}\left((1+\kappa)r + (1-\kappa)\dfrac{1}{r}\right)\right] & \text{if} \quad i = 1, 3, \\ \kappa_- \ln[4r^2h] + \ln\left[\dfrac{\kappa}{1-\kappa}\dfrac{l}{4h}\left\{(1-\kappa)\left(r+\dfrac{1}{r}\right)^2 + 4\kappa r^2\right\}\right] & \text{if} \quad i = 2. \end{cases} \tag{D.4}$$

Define the following utility difference functions at $\boldsymbol{h}^{**}$

$$\begin{aligned} v_{01}(r) \equiv & v_0(\boldsymbol{h}^{**}) - v_1(\boldsymbol{h}^{**}) \\ = & \kappa_- \ln\left[\frac{1}{r}\right] - \ln\left[\frac{1}{2}\left((1+\kappa)r + (1-\kappa)\frac{1}{r}\right)\right] \end{aligned} \tag{D.5}$$

$$\begin{aligned} v_{02}(r) \equiv & v_0(\boldsymbol{h}^{**}) - v_2(\boldsymbol{h}^{**}) \\ = & \kappa_- \ln\left[\frac{1}{r^2}\right] - \ln\left[\frac{1-\kappa}{4}\left(r+\frac{1}{r}\right)^2 + \kappa r^2\right] \end{aligned} \tag{D.6}$$

After a tedious calculation, we can show that

$$v_{0i} \begin{cases} < 0 & \text{for} \quad 0 < r < r_{0i}^{**}, \\ \geq 0 & \text{for} \quad r_{0i}^{**} \leq r < 1, \end{cases} \quad (i = 1, 2), \quad \text{and} \quad 0 < r_{01}^{**} < r_{02}^{**}, \tag{D.7}$$

where r_{0i}^{**} is the solution of $v_{0i}(r) = 0$ $(i = 1, 2)$. That is, the equilibrium condition for $\boldsymbol{h}^{**}$, $v_0(\boldsymbol{h}^{**}) = \max_k\{v_k(\boldsymbol{h}^{**})\}$, is satisfied for any r larger than r_{02}^{**}; that is, $r = r_{02}^{**}$ is the sustain point for $\boldsymbol{h}^{**}$.

E Proof of Lemma 5.1

The following two lemmas help us prove Lemma 5.1:

Lemma E.1 *All the submatrices $\boldsymbol{V}^{(ij)}$ defined in* (5.16) *are circulants.*

Lemma E.2 *The eigenvalues g_k^* $(k = 0, 1, 2, 3)$ of the Jacobian matrix $\nabla \boldsymbol{F}(\boldsymbol{h}^*)$ at $\boldsymbol{h}^* = [2h, 0, 2h, 0]^\top$ are represented as $g_2^* = e_1^{(00)}$, $g_0^* = -\bar{v}(\boldsymbol{h}^*)$ and $g_k^* = v_1(\boldsymbol{h}^*) - \bar{v}(\boldsymbol{h}^*)$ $(k =, 1, 3)$, where $\boldsymbol{e}^{(00)} \equiv [e_0^{(00)}, e_1^{(00)}]^\top$ denotes the eigenvalues of the Jacobian matrix $\boldsymbol{V}^{(00)}$.*

Proof of Lemma E.1:

As is shown in (3.36), the Jacobian matrix $\nabla \boldsymbol{v}(\boldsymbol{h}^*)$ consists of additions and multiplications of $\boldsymbol{M}(\boldsymbol{h}^*) \equiv \boldsymbol{D}\{\mathrm{diag}[\boldsymbol{D}^\top \boldsymbol{h}^*]\}$. It follows from this that the Jacobian matrix $D^\sharp \boldsymbol{v}(\boldsymbol{h}^*) \equiv \boldsymbol{P}\nabla \boldsymbol{v}(\boldsymbol{h}^*)\boldsymbol{P}^\top$ in the new coordinate system consists of those of $\boldsymbol{P}\boldsymbol{M}(\boldsymbol{h}^*)\boldsymbol{P}^\top$, which in turn is composed of submatrices $\boldsymbol{M}^{(ij)}$ $(i, j = 0, 1)$:

$$\boldsymbol{P}\boldsymbol{M}(\boldsymbol{h}^*)\boldsymbol{P}^\top \equiv \frac{1}{2h}\left[\begin{array}{c:c} \boldsymbol{M}^{(00)} & \boldsymbol{M}^{(01)} \\ \hdashline \boldsymbol{M}^{(01)} & \boldsymbol{M}^{(11)} \end{array}\right]. \tag{E.1}$$

Therefore, in order to prove that $\boldsymbol{V}^{(ij)}$ are circulants, it suffices to show that the submatrices $\boldsymbol{M}^{(ij)}$ are circulants. Note here that $\boldsymbol{P}M(\boldsymbol{h}^*)\boldsymbol{P}^\top$ can be represented as

$$\boldsymbol{P}\boldsymbol{M}(\boldsymbol{h}^*)\boldsymbol{P}^\top = \Big[\boldsymbol{P}\boldsymbol{D}\boldsymbol{P}^\top\Big]\Big[\boldsymbol{P}\{\mathrm{diag}[\boldsymbol{D}^\top\boldsymbol{h}^*]\}^{-1}\boldsymbol{P}^\top\Big]. \tag{E.2}$$

The first bracket of the right-hand side of (E.2) is given in (5.14), and a simple calculation of the second bracket yields

$$\boldsymbol{P}\{\mathrm{diag}[\boldsymbol{D}^\top\boldsymbol{h}^*]\}^{-1}\boldsymbol{P}^\top = \frac{1}{2h}\Big\{\mathrm{diag}[d_{(0)}, d_{(0)}, d_{(1)}, d_{(1)}]\Big\}^{-1} \tag{E.3}$$

where $d_{(0)} \equiv 1 + r^2$ and $d_{(1)} \equiv 2r$. Thus, we have

$$\boldsymbol{P}\boldsymbol{M}(\boldsymbol{h}^*)\boldsymbol{P}^\top = \frac{1}{2h}\begin{bmatrix}\boldsymbol{D}^{(0)}/d_{(0)} & \boldsymbol{D}^{(1)}/d_{(1)} \\ \boldsymbol{D}^{(1)}/d_{(0)} & \boldsymbol{D}^{(0)}/d_{(1)}\end{bmatrix} \tag{E.4}$$

which shows that the submatrices $\boldsymbol{M}^{(ij)}$ are circulants.

Proof of Lemma E.2: Consider the Jacobian matrix $\nabla^\sharp\boldsymbol{F}(\boldsymbol{h}^*) \equiv \boldsymbol{P}\nabla\boldsymbol{F}(\boldsymbol{h}^*)\boldsymbol{P}^\top$ in the new coordinate system:

$$\nabla^\sharp\boldsymbol{F}(\boldsymbol{h}^*) = \boldsymbol{J}^\sharp(\boldsymbol{h}^*) + \boldsymbol{\psi}^\sharp(\boldsymbol{h}^*)\nabla^\sharp\boldsymbol{v}(\boldsymbol{h}^*) \equiv \begin{bmatrix}\boldsymbol{F}^{(00)} & \boldsymbol{F}^{(01)} \\ \boldsymbol{F}^{(10)} & \boldsymbol{F}^{(11)}\end{bmatrix}, \tag{E.5}$$

where $\boldsymbol{J}^\sharp(\boldsymbol{h}^*) \equiv \boldsymbol{P}\boldsymbol{J}(\boldsymbol{h}^*)\boldsymbol{P}^\top$ and $\boldsymbol{\psi}^\sharp(\boldsymbol{h}^*) \equiv \boldsymbol{P}\boldsymbol{\psi}(\boldsymbol{h}^*)\boldsymbol{P}^\top$. Note here that the submatrices $\boldsymbol{F}^{(ij)}$ of the Jacobian matrix $\nabla^\sharp\boldsymbol{F}(\boldsymbol{h}^*)$ are circulants because all submatrices of $\boldsymbol{J}^\sharp(\boldsymbol{h}^*)$, $\boldsymbol{\psi}^\sharp(\boldsymbol{h}^*)$ and $\nabla^\sharp\boldsymbol{v}(\boldsymbol{h}^*)$ are circulants. This enables us to diagonalize each of the submatrices $\boldsymbol{F}^{(ij)}$ by using a 2-by-2 DFT matrix $\boldsymbol{Z}_{[2]}$:

$$\{\boldsymbol{Z}^\sharp\}^{-1}\nabla^\sharp\boldsymbol{F}\boldsymbol{Z}^\sharp = \begin{bmatrix}\mathrm{diag}[\boldsymbol{f}^{(00)}] & \mathrm{diag}[\boldsymbol{f}^{(01)}]] \\ \mathrm{diag}[\boldsymbol{f}^{(10)}] & \mathrm{diag}[\boldsymbol{f}^{(11)}]\end{bmatrix}, \tag{E.6}$$

where $\boldsymbol{f}^{(ij)}$ is the eigenvalues of $\boldsymbol{F}^{(ij)}$, and $\boldsymbol{Z}^\sharp \equiv \mathrm{diag}[\boldsymbol{Z}_{[2]}, \boldsymbol{Z}_{[2]}]$. It also follows that applying the similarity transformation based on $\boldsymbol{Z}_{[2]}$ to both sides of $\boldsymbol{F}^{(ij)}$ yields

$$\boldsymbol{f}^{(ij)} = \begin{cases}[\boldsymbol{1} - \boldsymbol{\delta}] \cdot [\boldsymbol{e}^{(ij)}] - \bar{v}\boldsymbol{\delta} & \text{if} \quad i = j = 0, \\ [\boldsymbol{1} - \boldsymbol{\delta}] \cdot [\boldsymbol{e}^{(ij)}] - v_1\boldsymbol{\delta} & \text{if} \quad i = 0, j = 1, \\ \boldsymbol{0} & \text{if} \quad i = 1, j = 0 \\ (v_1(\boldsymbol{h}^*) - \bar{v}(\boldsymbol{h}^*))\boldsymbol{1} & \text{if} \quad i = j = 1\end{cases} \tag{E.7}$$

where $\boldsymbol{\delta} \equiv [1, 0]^\top$ and $\boldsymbol{e}^{(ij)} \equiv [e_0^{(ij)}, e_1^{(ij)}]^\top$ denote the eigenvalues of $(1/2)\boldsymbol{E}$ and the Jacobian matrix $\boldsymbol{V}^{(ij)}$, respectively.

Therefore, (E.6) reduces to

$$\{\boldsymbol{Z}^\sharp\}^{-1}\nabla^\sharp \boldsymbol{F}\boldsymbol{Z}^\sharp = \left[\begin{array}{cc:cc} -\bar{v}(\boldsymbol{h}^*) & 0 & -v_1(\boldsymbol{h}^*) & 0 \\ 0 & e_1^{(00)} & 0 & e_1^{(01)} \\ \hdashline 0 & 0 & v_1(\boldsymbol{h}^*) - \bar{v}(\boldsymbol{h}^*) & 0 \\ 0 & 0 & 0 & v_1(\boldsymbol{h}^*) - \bar{v}(\boldsymbol{h}^*) \end{array}\right] \tag{E.8}$$

Converting this into the original coordinate system, we obtain

$$\begin{aligned} \boldsymbol{P}^\top \left[\{\boldsymbol{Z}^\sharp\}^{-1}\nabla^\sharp \boldsymbol{F}\boldsymbol{Z}^\sharp\right]\boldsymbol{P} &= \{\boldsymbol{Z}^\times\}^{-1}\nabla \boldsymbol{F}\boldsymbol{Z}^\times \\ &= \left[\begin{array}{cc:cc} -\bar{v}(\boldsymbol{h}^*) & -v_1(\boldsymbol{h}^*) & 0 & 0 \\ 0 & v_1(\boldsymbol{h}^*) - \bar{v}(\boldsymbol{h}^*) & 0 & 0 \\ \hdashline 0 & 0 & e_1^{(00)} & e_1^{(01)} \\ 0 & 0 & 0 & v_1(\boldsymbol{h}^*) - \bar{v}(\boldsymbol{h}^*) \end{array}\right], \end{aligned} \tag{E.9}$$

where $\boldsymbol{Z}^\times \equiv \boldsymbol{P}^\top \boldsymbol{Z}^\sharp \boldsymbol{P}$. Since eigenvalues of an upper-triangular matrix are given by the diagonal entries, we can conclude that the eigenvalues of the Jacobian $\nabla \boldsymbol{F}(\boldsymbol{h}^*)$ are given by $[-\bar{v}(\boldsymbol{h}^*), v_1(\boldsymbol{h}^*) - \bar{v}(\boldsymbol{h}^*), \theta e_1^{(00)}, v_1(\boldsymbol{h}^*) - \bar{v}(\boldsymbol{h}^*)]^\top$.

Proof of Lemma 5.1: Substituting (3.36) and (E.4) into the definition of $\nabla^\sharp \boldsymbol{v}(\boldsymbol{h}^*)$ in (5.16), we see that the Jacobian matrix $\boldsymbol{V}^{(00)}$ consists of additions and multiplications of $\boldsymbol{D}^{(0)}$ and $\boldsymbol{D}^{(1)}$:

$$\boldsymbol{V}^{(00)} \equiv \left[\boldsymbol{I} - \kappa\left(\frac{\boldsymbol{D}^{(0)}}{d_{(0)}}\right)\right]^{-1}\left[b\left[\frac{\boldsymbol{D}^{(0)}}{d_{(0)}}\right] - \left\{a^*\left[\frac{\boldsymbol{D}^{(0)}}{d_{(0)}}\right]^2 + a^*_{(1)}\left[\frac{\boldsymbol{D}^{(1)}}{d_{(1)}}\right]^2\right\}\right], \tag{E.10}$$

where $d_{(0)} \equiv 1 + r^2$, $d_{(1)} \equiv 2r$, $a^* \equiv \kappa\kappa_- + (1+\kappa)/2$, $a^*_{(1)} \equiv (1-\kappa)/2$ and $b \equiv \kappa + \kappa_-$. Since $\boldsymbol{D}^{(0)}$ and $\boldsymbol{D}^{(1)}$ are circulants, we have the following expressions for the eigenvalues $\boldsymbol{e}^{(00)}$ of the Jacobian $\boldsymbol{V}^{(00)}$:

$$e_k^{(00)} = \frac{b f_k^{(0)} - \{a^*[f_k^{(0)}]^2 + a^*_{(1)}[f_k^{(1)}]^2\}}{1 - \kappa f_k^{(0)}}, \tag{E.11}$$

where $f_k^{(i)}$ $(i = 0, 1)$ is the k-th eigenvalue of $\boldsymbol{D}^{(i)}/d_{(i)}$, which is obtained by DFT of vectors $\boldsymbol{d}_0^{(i)}$:

$$\boldsymbol{f}_{(0)} = \frac{1}{d_{(0)}}\boldsymbol{Z}_{[2]}\{\boldsymbol{d}_0^{(0)}\}^\top = \frac{1}{1+r^2}\begin{bmatrix}1 & 1\\ 1 & -1\end{bmatrix}\begin{bmatrix}1\\ r^2\end{bmatrix} = \begin{bmatrix}1\\ c(r^2)\end{bmatrix}, \tag{E.12a}$$

$$\boldsymbol{f}_{(1)} = \frac{1}{d_{(1)}}\boldsymbol{Z}_{[2]}\{\boldsymbol{d}_0^{(1)}\}^\top = \frac{1}{2r}\begin{bmatrix}1 & 1\\ 1 & -1\end{bmatrix}\begin{bmatrix}r\\ r\end{bmatrix} = \begin{bmatrix}1\\ 0\end{bmatrix} \tag{E.12b}$$

Substituting (E.12) into (E.11) yields

$$e_0^{(00)} = -1 + \kappa_-, \quad e_1^{(00)} = \frac{bx - a^* x^2}{1 - \kappa x}, \quad \text{where} \quad x \equiv c(r^2) \tag{E.13}$$

Combining (E.13) and Lemma E.2, we obtain Lemma 5.1.

F Proof of Lemma 6.1

Suppose that $\boldsymbol{h}_2$ is an equilibrium (i.e., $v_0(\boldsymbol{h}_2) = v_1(\boldsymbol{h}_2)$). Then, we have

$$R(\nabla \boldsymbol{F}(\boldsymbol{h}_2), \boldsymbol{z}_1^\top) = \frac{-(1-\mu) + (\kappa + \kappa_-)(1-r^2)\eta - \mu\kappa_-(1-r^2)^2\eta^2 - \{\sigma^{-1} - (1-\mu)\}\left[1 + r^2 - 2r\left(\frac{w_1}{w_0}\right)^\sigma\right]\eta}{1 - \left\{\frac{\kappa}{\kappa_-}\left[1 + r^2 - 2r\left(\frac{w_1}{w_0}\right)^\sigma\right] + \kappa(1-r^2)\right\}\eta}, \tag{F.1}$$

where $\eta \equiv (w_0^{1-\sigma} h_0)/\tilde{\Delta}_0 < 1$. The following lemma helps in proving that the Rayleigh quotient $R(\nabla \boldsymbol{F}(\boldsymbol{h}_2), \boldsymbol{z}_1^\top)$ is positive.

Lemma F.1 *If the duo-centric pattern $\boldsymbol{h}_2 = [h_0, h_1, h_0, h_1]^\top$ ($h_0 > h_1$) is an equilibrium of the Hm model, $w_0 - w_1$ and $w_0^{1-\sigma} h_0 - w_1^{1-\sigma} h_1$ are positive.*

Proof For the duo-centric pattern $\boldsymbol{h}_2$, we can rewrite the wage equations (3.25b) as

$$w_0 = \mu w_0^{1-\sigma}\left\{\frac{(1+r^2)(w_0+1)h_0}{\tilde{\Delta}_0} + \frac{2r(w_1+1)(H/2-h_0)}{\tilde{\Delta}_1}\right\}, \tag{F.2a}$$

$$w_1 = \mu w_1^{1-\sigma}\left\{\frac{2r(w_0+1)h_0}{\tilde{\Delta}_0} + \frac{(1+r^2)(w_1+1)(H/2-h_0)}{\tilde{\Delta}_1}\right\}, \tag{F.2b}$$

$$\tilde{\Delta}_0 = (1+r^2)w_0^{1-\sigma}h_0 + 2rw_1^{1-\sigma}(H/2-h_0), \tag{F.2c}$$

$$\tilde{\Delta}_1 = 2rw_0^{1-\sigma}h_0 + (1+r^2)w_1^{1-\sigma}(H/2-h_0). \tag{F.2d}$$

This yields the relationship between $w_0 - w_1$ and $w_0^{1-\sigma} h_0 - w_1^{1-\sigma} h_1$:

$$\begin{aligned}&\mu r H(w_0+1)w_0^{1-\sigma}(1-r)^2\left(w_0^{1-\sigma}h_0 - w_1^{1-\sigma}h_1\right)\\ &\quad = \left\{\tilde{\Delta}_0\tilde{\Delta}_1(1-\mu) + \mu r H w_0^{1-\sigma}\tilde{\Delta}_0\right\}(w_0 - w_1) - \mu r H(w_0+1)\tilde{\Delta}_1\left(w_0^{1-\sigma} - w_1^{1-\sigma}\right).\end{aligned} \tag{F.3}$$

Because $-(w_0^{1-\sigma} - w_1^{1-\sigma})$ and $(w_0 - w_1)$ have the same sign, $w_0 - w_1$ and $w_0^{1-\sigma} h_0 - w_1^{1-\sigma} h_1$ also have the same sign. Moreover, the equilibrium condition for the duo-centric pattern is rewritten as

$$\frac{\mu}{\sigma - 1}\ln\left[\frac{\tilde{\Delta}_0}{\tilde{\Delta}_1}\right] + \mu \ln\left[\frac{w_0+1}{w_1+1}\right] = (1-\mu)\ln\left[\frac{h_0}{h_1}\right] > 0. \tag{F.4}$$

This condition implies that $w_0 - w_1$ and/or $\tilde{\Delta}_0 - \tilde{\Delta}_1 = (1-r)^2(w_0^{1-\sigma} h_0 - w_1^{1-\sigma} h_1)$ must be

positive. Thus, from (F.3) and (F.4), $w_0 - w_1$ and $\tilde{\Delta}_0 - \tilde{\Delta}_1 = (1-r)^2(w_0^{1-\sigma}h_0 - w_1^{1-\sigma}h_1)$ are positive if the duo-centric pattern $\boldsymbol{h}_2$ is an equilibrium. □

From Lemma F.1 and the wage equations (3.25b), we have

$$(1-r^2)\eta > f_1(r), \tag{F.5a}$$

$$\mu(h_0+h_1) = (1-\mu)(w_0h_0 + w_1h_1) < (1-\mu)w_0(h_0+h_1). \tag{F.5b}$$

Combining (3.25b) with (F.5b), we obtain

$$1 + r^2 - 2r\left(\frac{w_1}{w_0}\right)^{\sigma} = \frac{\mu(1-r)^2(w_0+1)w_0^{-\sigma}h_0}{\tilde{\Delta}_0} < (1-r^2)^2\eta. \tag{F.6}$$

It follows from this and (6.4) that the Rayleigh quotient $R(\nabla \boldsymbol{F}(\boldsymbol{h}_2), \boldsymbol{z}_1^{\top})$ satisfies the following condition:

$$R(\nabla \boldsymbol{F}(\boldsymbol{h}_2), \boldsymbol{z}_1^{\top}) > \frac{-(1-\mu) + b(1-r^2)\eta - \tilde{a}(1-r^2)^2\eta^2}{1 - \left\{\frac{\kappa}{\kappa_-}\left[1 + r^2 - 2r\left(\frac{w_1}{w_0}\right)^{\sigma}\right] + \kappa(1-r^2)\right\}\eta}. \tag{F.7}$$

Because $-(1-\mu) + bx - \tilde{a}x^2 > 0$ for any x larger than $\tilde{x}_-^*$ (Figure 3 (b)) and the condition (F.5a) holds,

$$\frac{-(1-\mu) + b(1-r^2)\eta - \tilde{a}(1-r^2)^2\eta^2}{1 - \left\{\frac{\kappa}{\kappa_-}\left[1 + r^2 - 2r\left(\frac{w_1}{w_0}\right)^{\sigma}\right] + \kappa(1-r^2)\right\}\eta} > 0 \quad \text{if} \quad f_1(r) > \tilde{x}_-^*. \tag{F.8}$$

Therefore, we obtain (6.9).

References

Akamatsu, T., Takayama, Y., Ikeda, K., 2012. Spatial discounting, Fourier, and racetrack economy: A recipe for the analysis of spatial agglomeration models. Journal of Economic Dynamics and Control 36 (11), 1729–1759.

Allen, T., Arkolakis, C., 2014. Trade and the topography of the spatial economy. The Quarterly Journal of Economics 129 (3), 1085–1140.

Baldwin, R. E., Forslid, R., Martin, P., Ottaviano, G. I. P., Robert-Nicoud, F., 2003. Economic Geography and Public Policy. Princeton University Press.

Behrens, K., Mion, G., Murata, Y., Südekum, J., 2014. Spatial frictions. Discussion Paper No.160, Düsseldorf Institute for Competition Economics.

Behrens, K., Murata, Y., 2007. General equilibrium models of monopolistic competition: A new approach. Journal of Economic Theory 136 (1), 776–787.

Behrens, K., Robert-Nicoud, F., 2015. Agglomeration theory with heterogeneous agents. In: Duranton, G., Henderson, J. V., Strange, W. C. (Eds.), Handbook of Regional and Urban Economics. Vol. 5. Elsevier B.V., pp. 171–245.

Caliendo, L., Parro, F., Rossi-hansberg, E., Sarte, P.-D., 2015. The impact of regional and sectoral productivity changes on the U.S. economy. manuscript.

Combes, P.-P., Gobillon, L., 2015. The empirics of agglomeration economies. In: Duranton, G., Henderson, J. V., Strange, W. C. (Eds.), Handbook of Regional and Urban Economics. Vol. 5. Elsevier B.V., pp. 247–348.

Cottle, R. W., Pang, J.-S., Stone, R. E., 2009. The Linear Complementarity Problem. SIAM.

Desmet, K., Ghani, E., O'Connell, S., Rossi-Hansberg, E., 2015a. The spatial development of India. Journal of Regional Science 55 (1), 10–30.

Desmet, K., Nagy, D. K., Rossi-Hansberg, E., 2015b. The geography of development: Evaluating migration restrictions and coastal flooding. manuscript.

Desmet, K., Rossi-Hansberg, E., 2009. Spatial growth and industry age. Journal of Economic Theory 144 (6), 2477–2502.

Desmet, K., Rossi-Hansberg, E., 2013. Urban accounting and welfare. American Economic Review 103 (6), 2296–2327.

Desmet, K., Rossi-Hansberg, E., 2014. Spatial development. American Economic Review 104 (4), 1211–1243.

Desmet, K., Rossi-Hansberg, E., 2015. On the spatial economic impact of global warming. Journal of Urban Economics 88, 16–37.

Duranton, G., Puga, D., 2004. Micro-foundations of urban agglomeration economies. In: Henderson, J. V., Thisse, J.-F. (Eds.), Handbook of Regional and Urban Economics. Vol. 4. Elsevier, pp. 2063–2117.

Fabinger, M., 2015. Cities as solitons: Analytic solutions to models of agglomeration and related numerical approaches. manuscript.

Facchinei, F., Pang, J.-S., 2003. Finite-dimensional Variational Inequalities and Complementarity Problems. Springer.

Forslid, R., 1999. Agglomeration with human and physical capital: An analytically solvable case.

Forslid, R., Ottaviano, G. I. P., 2003. An analytically solvable core-periphery model. Journal of Economic Geography 3 (3), 229–240.

Fujita, M., Krugman, P. R., 1995. When is the economy monocentric?: von Thünen and Chamberlin unified. Regional Science and Urban Economics 25 (4), 505–528.

Fujita, M., Krugman, P. R., Venables, A. J., 1999. The Spatial Economy: Cities, Regions and International Trade. MIT Press.

Golubitsky, M., Stewart, I., Schaeffer, D., 1988. Singularities and Groups in Bifurcation Theory. Springer-Verlag.

Gray, R. M., 2006. Toeplitz and Circulant Matrices: A Review. Now Publishers.

Hale, J. K., Koçak, H., 1991. Dynamics and Bifurcations. Springer-Verlag.

Hawkins, D., Simon, H. A., 1949. Note: some conditions of macroeconomic stability. Econometrica 17 (3), 245–248.

Helpman, E., 1998. The size of regions. In: Pines, D., Sadka, E., Zilcha, I. (Eds.), Topics in Public Economics: Theoretical and Applied Analysis. Cambridge: Cambridge University Press, pp. 33–54.

Henderson, J. V., 1974. The sizes and types of cities. American Economic Review 64 (4), 640–656.

Hirsch, M. W., Smale, S., 1974. Differential Equations, Dynamical Systems, and Linear Algebra. Academic Press.

Horn, R. A., Johnson, C. R., 2013. Matrix Analysis, 2nd Edition. Cambridge University Press.

Hsu, W.-T., 2012. Central place theory and city size distribution. The Economic Journal 122 (563), 903–932.

Ikeda, K., Akamatsu, T., Kono, T., 2012a. Spatial period-doubling agglomeration of a core-periphery model with a system of cities. Journal of Economic Dynamics and Control 36 (5), 754–778.

Ikeda, K., Murota, K., 2010. Imperfect Bifurcation in Structures and Materials. Springer.

Ikeda, K., Murota, K., 2014. Bifurcation Theory for Hexagonal Agglomeration in Economic Geography. Springer.

Ikeda, K., Murota, K., Akamatsu, T., 2012b. Self-organization of Lösch's hexagons in economic agglomeration for core-periphery models. International Journal of Bifurcation and Chaos 22 (08).

Ikeda, K., Murota, K., Akamatsu, T., Kono, T., Takayama, Y., 2014. Self-organization of hexagonal agglomeration patterns in new economic geography models. Journal of Economic Behavior and Organization 99, 32–52.

Ikeda, K., Murota, K., Akamatsu, T., Takayama, Y., 2015. Agglomeration patterns in a long narrow economy of a new economic geography model: Analogy to a racetrack economy. mimeograph.

Krugman, P. R., 1991. Increasing returns and economic geography. The Journal of Political Economy 99 (3), 483–499.

Krugman, P. R., 1996. The Self-organizing Economy. Blackwell Publishers.

Mossay, P., 2003. Increasing returns and heterogeneity in a spatial economy. Regional Science and Urban Economics 33 (4), 419–444.

Murata, Y., 2003. Product diversity, taste heterogeneity, and geographic distribution of economic activities: market vs. non-market interactions. Journal of Urban Economics 53 (1), 126–144.

Murata, Y., Thisse, J.-F., 2005. A simple model of economic geography à la Helpman-Tabuchi. Journal of Urban Economics 58 (1), 137–155.

Nakajima, K., 2008. Economic division and spatial relocation: The case of postwar Japan. Journal of the Japanese and International Economies 22 (3), 383–400.

Nikaido, H., 1968. Convex Structures and Economic Theory. Vol. 51. Academic Press.

Osawa, M., Akamatsu, T., Takayama, Y., 2015. Harris and Wilson (1978) model revisited: Spatial period doubling bifurcation cascade in an urban retail model. mimeograph.

Ottaviano, G. I. P., 1996. Monopolistic competition, trade, and endogenous spatial fluctuation. Discussion paper 1327, Centre for Economic Policy Research, London.

Ottaviano, G. I. P., 2001. Monopolistic competition, trade, and endogenous spatial fluctuations. Regional Science and Urban Economics 31 (1), 51–77.

Ottaviano, G. I. P., Tabuchi, T., Thisse, J.-F., 2002. Agglomeration and trade revisited. International Economic Review 43 (2), 409–435.

Oyama, D., 2009. Agglomeration under forward-looking expectations: Potentials and global stability. Regional Science and Urban Economics 39 (6), 696–713.

Papageorgiou, Y. Y., Smith, T. R., 1983. Agglomeration as local instability of spatially uniform steady-states. Econometrica 51 (4), 1109–1119.

Pflüger, M., 2004. A simple, analytically solvable, Chamberlinian agglomeration model. Regional Science and Urban Economics 34 (5), 565–573.

Pflüger, M., Südekum, J., 2010. The size of regions with land use for production. Regional Science and Urban Economics 40 (6), 481–489.

Picard, P. M., Tabuchi, T., 2010. Self-organized agglomerations and transport costs. Economic Theory 42 (3), 565–589.

Redding, S. J., 2015. Goods trade, factor mobility and welfare. mimeograph.

Redding, S. J., Sturm, D. M., 2008. The costs of remoteness: Evidence from German division and reunification. American Economic Review 98 (5), 1766–1797.

Rosenthal, S. S., Strange, W. C., 2004. Evidence on the nature and sources of agglomeration economies. In: Henderson, J. V., Thisse, J.-F. (Eds.), Handbook of Regional and Urban Economics. Elsevier, pp. 2119–2171.

Sandholm, W. H., 2010. Population Games and Evolutionary Dynamics. MIT Press.

Stewart, I., 2013. Symmetry—A Very Short Introduction. Oxford University Press.

Strogatz, S. H., 2014. Nonlinear Dynamics and Chaos: With Applications to Physics, Biology, Chemistry, and Engineering, second edi Edition. Westview Press.

Tabuchi, T., 1998. Urban agglomeration and dispersion: a synthesis of Alonso and Krugman. Journal of Urban Economics 44 (3), 333–351.

Tabuchi, T., Thisse, J.-F., 2002. Taste heterogeneity, labor mobility and economic geography. Journal of Development Economics 69 (1), 155–177.

Tabuchi, T., Thisse, J.-F., 2011. A new economic geography model of central places. Journal of Urban Economics 69 (2), 240–252.

Tabuchi, T., Thisse, J.-F., Zeng, D.-Z., 2005. On the number and size of cities. Journal of Economic Geography 5 (4), 423–448.

Takayama, Y., Akamatsu, T., 2011. Emergence of polycentric urban configurations from combination of communication externality and spatial competition. Journal of Japan Society of Civil Engineers, Series D3 (Infrastructure Planning and Management) 67 (1), 1–20 (in Japanese).

Turing, A. M., 1952. The chemical basis of morphogenesis. Philosophical Transactions of the Royal Society of London. Series B, Biological Sciences 237 (641), 37–72.

Weibull, J. W., 1995. Evolutionary Game Theory. MIT Press.